ORNL/SUB/99-19XSY063V-1

ornl

OAK RIDGE
NATIONAL
LABORATORY

LOCKHEED MARTIN

Evaluation of Mixed LEU-MOX Loading Patterns for LWRs Originating from Inability to Deliver MOX Assemblies

(ABB–CE System 80 Reload Core Study)

Imelda Ariani
Paul J. Turinsky

MANAGED AND OPERATED BY
LOCKHEED MARTIN ENERGY RESEARCH CORPORATION
FOR THE UNITED STATES
DEPARTMENT OF ENERGY

ORNL-27 (3-96)

This report was prepared as an account of work sponsored by an agency of the United States Government. Neither the United States Government nor any agency thereof, nor any of their employees, makes any warranty, express or implied, or assumes any legal liability or responsibility for the accuracy, completeness, or usefulness of any information, apparatus, product, or process disclosed, or represents that its use would not infringe privately owned rights. Reference herein to any specific commercial product, process, or service by trade name, trademark, manufacturer, or otherwise, does not necessarily constitute or imply its endorsement, recommendation, or favoring by the United States Government or any agency thereof. The views and opinions of authors expressed herein do not necessarily state or reflect those of the United States Government or any agency thereof.

ORNL/SUB/99-19XSY063V-1

EVALUATION OF MIXED LEU-MOX LOADING PATTERNS FOR LWRs ORIGINATING FROM INABILITY TO DELIVER MOX ASSEMBLIES

(ABB–CE System 80 Reload Core Study)

Authors

Imelda Ariani
Paul J. Turinsky

Date Published: February 1999

Report Prepared by
LOCKHEED MARTIN ENERGY RESEARCH CORP.
P.O. Box 2008
Oak Ridge, Tennessee 37831-6363
under
Subcontract Number 85B99398V

Funded by
Office of Fissile Materials Disposition
United States Department of Energy

Prepared for
Computational Physics and Engineering Division
Oak Ridge National Laboratory
Oak Ridge, Tennessee 37831
managed by
LOCKHEED MARTIN ENERGY RESEARCH CORP.
for the
U.S. DEPARTMENT OF ENERGY
under contract DE-96OR22464

FINAL REPORT

Evaluation of Mixed LEU-MOX Loading Patterns for LWRs Originating from Inability to Deliver MOX Assemblies

ABB-CE System 80 Reload Core Study

Imelda Ariani and Paul J. Turinsky

Electric Power Research Center
Department of Nuclear Engineering
North Carolina State University
Raleigh, NC

October, 1998

Contents

1. Introduction 1

2. Methodology 2

3. Lattice Physics Predictions 3

4. HELIOS/FORMOSA-P versus DIT/ROCS Predictions for Full MOX Core 21

5. Initial Mixed Core 28

6. Subsequent Mixed LEU-MOX Cores 34

   6.1 Scenario 1: MOX Feed Batches Available for Subsequent Cycle 34

   6.2 Scenario 2: MOX Feed Batches Continue to be Unavailable for Subsequent Cycle 47

   6.3 Scenario 3: Only One MOX Feed Batch is Available (Dominant Batch) for Subsequent Cycle 53

7. Conclusions 55

8. Acknowledgment 55

9. References 56

List of Figures

FIGURE 1. 24 UO2 - Er2O3 Rod MOX Assembly "Low Enrichment" BOL Rel. Pin Power Dist. 15

FIGURE 2. 24 UO2 - Er2O3 Rod MOX Assembly "High Enrichment" BOL Rel. Pin Power Dist. 15

FIGURE 3. 48 UO2 - Er2O3 Rod MOX Assembly "Low Enrichment" BOL Rel. Pin Power Dist. 16

FIGURE 4. 48 UO2 - Er2O3 Rod MOX Assembly "High Enrichment" BOL Rel. Pin Power Dist. 16

FIGURE 5. 56 UO2 - Er2O3 Rod MOX Assembly "Low Enrichment" BOL Rel. Pin Power Dist. 17

FIGURE 6. 56 UO2 - Er2O3 Rod MOX Assembly "High Enrichment" BOL Rel. Pin Power Dist. 17

FIGURE 7. 60 UO2 - Er2O3 Rod MOX Assembly "Low Enrichment" BOL Rel. Pin Power Dist. 18

FIGURE 8. 60 UO2 - Er2O3 Rod MOX Assembly "High Enrichment" BOL Rel. Pin Power Dist. 18

FIGURE 9. 72 UO2 - Er2O3 Rod MOX Assembly "Low Enrichment" BOL Rel. Pin Power Dist. 19

FIGURE 10. 72 UO2 - Er2O3 Rod MOX Assembly "High Enrichment" BOL Rel. Pin Power Dist. 19

FIGURE 11. kinf Differences for Various ABB-CE MOX Lattices 20

FIGURE 12. Equilibrium Cycle, Full MOX Core Loading Pattern 23

FIGURE 13. CASE2:EquilibriumCycle,FullMOXCoreBOCAssemblyBurnupDistribution 24

FIGURE 14. CASE2:EquilibriumCycle,FullMOXCoreBOCAssemblyPowerDistribution 25

FIGURE 15. CASE 2: Equilibrium Cycle, Full MOX Core BOC Assembly Distribution 25

FIGURE 16. CASE2:EquilibriumCycle,FullMOXCoreEOCAssemblyBurnupDistribution 26

FIGURE 17. CASE2:EquilibriumCycle,FullMOXCoreEOCAssemblyPowerDistribution 26

List of Figures

FIGURE 18. CASE 2: Equilibrium Cycle, Full MOX Core EOC Assembly Distribution 27

FIGURE 19. Example of ABB-CE Standard LEU Lattice Designs 30

FIGURE 20. Initial Mixed Core Loading Pattern 31

FIGURE 21. Initial Mixed Core BOC Conditions 32

FIGURE 22. Initial Mixed Core EOC Conditions 32

FIGURE 23. kinf versus Burnup for MOX and LEU Assemblies 33

FIGURE 24. MOX assembly reactivity versus burnup for different WGPu average assembly enrichments and BP loadings 39

FIGURE 25. Scenario 1.a Loading Pattern 40

FIGURE 26. Scenario 1.a Core BOC Conditions 41

FIGURE 27. Scenario 1.a Pin-Wise Power Distribution 41

FIGURE 28. Scenario 1.a Core EOC Conditions 42

FIGURE 29. Scenario 1.a Pin-Wise Discharge Burnup Distribution 42

FIGURE 30. Scenario 1.b Core Loading Pattern 43

FIGURE 31. Scenario 1.b Core BOC Conditions 44

FIGURE 32. Scenario 1.b Core EOC Conditions 44

FIGURE 33. Scenario 1.c Core Loading Pattern 45

FIGURE 34. Scenario 1.c Core BOC Conditions 46

FIGURE 35. Scenario 1.c EOC Conditions 46

FIGURE 36. Scenario 2.a Loading Pattern 48

FIGURE 37. Scenario 2.a Core BOC Conditions 49

FIGURE 38. Scenario 2.a Core EOC Conditions 49

FIGURE 39. Scenario 2.a: Pin-Wise Discharge Burnup Distribution 50

FIGURE 40. Scenario 2.b Loading Pattern 51

FIGURE 41. Scenario 2.b Core BOC Conditions 52

FIGURE 42. Scenario 2.b Core EOC Conditions 52

FIGURE 43. Scenario 3 Core BOC Conditions 54

FIGURE 44. Scenario 3 Core EOC Conditions 54

List of Tables

TABLE 1: 24 UO2 - Er2O3 Rod MOX Assembly "Low Enrichment" Comparisons 5

TABLE 2: 24 UO2 - Er2O3 Rod MOX Assembly "High Enrichment" Comparisons 6

TABLE 3: 48 UO2 - Er2O3 Rod MOX Assembly "Low Enrichment" Comparisons 7

TABLE 4: 48 UO2 - Er2O3 Rod MOX Assembly "High Enrichment" Comparisons 8

TABLE 5: 56 UO2 - Er2O3 Rod MOX Assembly "Low Enrichment" Comparisons 9

TABLE 6: 56 UO2 - Er2O3 Rod MOX Assembly "High Enrichment" Comparisons 10

TABLE 7: 60 UO2 - Er2O3 Rod MOX Assembly "Low Enrichment" Comparisons 11

TABLE 8: 60 UO2 - Er2O3 Rod MOX Assembly "High Enrichment" Comparisons 12

TABLE 9: 72 UO2 - Er2O3 Rod MOX Assembly "Low Enrichment" Comparisons 13

TABLE 10: 72 UO2 - Er2O3 Rod MOX Assembly "High Enrichment" Comparisons 14

TABLE 11: Baffle/Reflector ADFs for Various MOX Lattices and LEU Lattice 20

TABLE 12: Baffle/Reflector Diffusion Coefficients for Various MOX Lattices and LEU Lattice 21

TABLE 13: CASE 2 Equilibrium Cycle, Full MOX Core Feed Batches 23

TABLE 14: CASE 2 Equilibrium Cycle, Full MOX Core Performance Characteristics Predictions for DIT/ROCS vs. HELIOS/FORMOSAP 24

TABLE 15: Initial Mixed Core Feed Batches 30

TABLE 16: CASE 2 Full MOX & Initial Mixed Cores Performance Characteristics 30

TABLE 17: Various Scenarios' Mixed LEU-MOX Cores Performance Characteristics 39

1. Introduction

This study is in support of the weapon's grade Pu disposition project utilizing the reactor option, which entails burning weapon's grade Mixed Oxide (MOX) fuel in Light Water Reactors (LWRs). What is being evaluated is the feasibility of substituting Low Enriched Uranium (LEU) fuel assemblies for weapon's grade MOX assemblies starting from an equilibrium cycle, full MOX core. The specific focus of this report is on the ABB-CE System 80 Pressurized Water Reactor (PWR) core design, starting with an equilibrium cycle, full MOX core identified by ABB-CE [1]. The motivation for this study is two fold. Firstly, since there are technical and political uncertainties associated with the utilization of weapon's grade MOX assemblies, there is a potential that some or all of the feed fuel assemblies associated with a reload region may not be available in a timely manner. This condition will be referred to as the disruption scenario. Secondly, at the conclusion of the Pu disposition campaign, the reactors involved will need to transition back to full LEU cores. Either condition will result in the insertion of feed LEU assemblies in a core containing once and twice burnt weapon's grade MOX assemblies. There are known design challenges associated with mixed LEU-MOX cores. Work to date has addressed transitioning from an equilibrium cycle, full LEU core to an equilibrium cycle, full MOX core. The emphasis of the current study is noted to be related to the reverse transition, with the additional complexity of not knowing when this will occur for the disruption scenario.

The design features of interest include the lattice design and core loading pattern (LP). The lattice design involves the placement of fuel and burnable poison (BP) material within the fuel lattice. In all cases, the ABB-CE Erbia integral BP design has been employed. Since integral BPs have not been utilized with MOX pellets, DOE has restricted integral BP usage to LEU pellets, which ABB-CE has addressed for MOX assemblies by displacing some MOX pins with Erbia (with U) pins. The lattice designs used in this study for both MOX and LEU lattices have been restricted to existing ABB-CE designs, with lattice average enrichment and BP loading, *i.e.* number of BP rods, as free decision variables. In determining the LP, most active LP constraints have been imposed, the exception being the shutdown margin constraint.

2. Methodology

To complete the mixed LEU-MOX core assessment, core simulator models must be established. This involves generating two-group, homogenized cross-sections via a lattice physics code and solving the two-group neutron diffusion equation via a core simulator code. The lattice physics code that was employed in this study is the HELIOS code [2]. HELIOS employs the Current Coupling Collision Probability (CCCP) method to solve the integral form of the neutron transport equation. The many-group cross-section library is based upon ENDF/B-VI. The resonance treatment employs the subgroup method. The core simulator that was employed is the FORMOSA-P code [3]. FORMOSA-P solves the two-dimensional (radial), two-group neutron diffusion equation utilizing the Nodal Expansion Method (NEM) based upon quartic polynomials. The microscopic depletion option of FORMOSA-P has been utilized to better represent interfacial effects at LEU-MOX assembly interfaces. Pin-power reconstruction is completed utilizing intra-nodal fluxes and pin-power form factors, correcting for spatially dependent, spectral history effects. Pin burnups are evaluated based solely upon the intra-nodal burnup distribution. The unique feature of FORMOSA-P is the incorporation of a mathematical optimization capability to determine the near-optimum LPs for a stated objective function within imposed constraints. This is done utilizing the simulated annealing, stochastic optimization method and adaptive penalty functions. In determining the LP, the feed enrichment and BP loadings of the feed assemblies are also determined to satisfy cycle energy requirement and maximum soluble boron limit, respectively. The objective utilized throughout most of this study is the minimization of the feed enrichment of the dominant feed batch, this objective function being a surrogate for minimizing the feed region cost.

To link HELIOS to FORMOSA-P, the ZENITH [2] and FORCIP-P [4] codes were employed. ZENITH can read and process the output files of HELIOS as directed by user input provided in a higher level language, *e.g.* mathematical formulas. FORCIP-P was modified to read the ZENITH output file, manipulate the cross-sections to the form required by FORMOSA-P, and create the FORMOSA-P cross-section input file.

3. Lattice Physics Predictions

HELIOS lattice physics calculations were completed for a range of MOX and LEU lattice designs, spanning different fuel enrichments and BP loadings. This provided the lattice design inventory from which FORMOSA-P selected, with fuel enrichment treated as a continuous decision variable and BP loading as an integer decision variable. For each lattice design, the lattice was depleted to high burnup at base case conditions, *i.e.* Hot Full Power (HFP) average moderator density and fuel temperature. Multiple instantaneous branch cases were executed during the depletion, enabling characterization of the cross-sections as a function of moderator density, fuel temperature and soluble boron concentration within FORMOSA-P in order to apply spatially dependent, feedback corrections.

Table 1 through Table 10 show the k_∞ prediction comparisons between HELIOS and DIT, the ABB-CE lattice physics code, for base case conditions for the ten MOX lattice designs developed by ABB-CE [1]. Figure 1 through Figure 10 show the BOL relative pin power distribution comparisons for these lattices. Note that results presented for HELIOS use ten uniform radial regions per pin cell and three angular sectors. The trend of HELIOS predicting higher k_∞ values at lower burnups and lower k_∞ values at higher burnups versus DIT predictions is common to all lattices. In no case does the difference in k_∞ between HELIOS and DIT exceed 0.0055, which is judged to be very good for heavily loaded MOX lattices. The k_∞ agreement at BOL is better for lattices with higher number of UO_2-Er_2O_3 rods (Figure 11). For the same number of UO_2-Er_2O_3 rods, the "high enrichment" lattices give better agreements than the "low enrichment" lattices.

Lattice physics calculations were also completed for non-fuel lattices; in particular, for the Baffle/Reflector lattice as depicted above Table 11. One concern addressed was the sensitivity of the Baffle/Reflector cross-sections to the fuel lattice adjacent to the baffle. Table 11 and Table 12 show that Baffle/Reflector Assembly Discontinuity Factor (ADF) and diffusion coefficient values are fairly insensitive to the MOX lattice selection. This is important, since FORMOSA-P currently only allows one set of two-group data to be assigned to the Baffle/Reflector. Similar results are obtained for MOX versus LEU, except for the thermal ADF at the Region I fuel/baffle interface. This difference is not due to the

thermal diffusion coefficient, since the D_2 value for MOX versus LEU is similar, implying substantial differences in the spatial distribution of the thermal flux about the Region I fuel/baffle interface. For mixed MOX-LEU cores, when both MOX and LEU assemblies can be located on core peripheral locations, this sensitivity could be a source of error in FORMOSA-P predictions given the current restriction of only allowing one set of two-group data to be assigned to the Baffle/Reflector.

TABLE 1: 24 UO_2 - Er_2O_3 Rod MOX Assembly "Low Enrichment" k_∞ Comparisons

Time (days)	Exposure (MWd/MT)	DIT	HELIOS	DIT - HELIOS
0	0	1.22036	1.22427	-0.0039
1.4	50	1.19768	1.19959	-0.0019
13.8	500	1.18718	1.19104	-0.0039
27.6	1000	1.18003	1.18377	-0.0037
55.2	2000	1.16930	1.17264	-0.0033
82.8	3000	1.16044	1.16335	-0.0029
138.0	5000	1.14511	1.14712	-0.0020
193.2	7000	1.13106	1.13211	-0.0010
248.4	9000	1.11783	1.11805	-0.0002
303.6	11000	1.10519	1.10465	0.0005
386.4	14000	1.08732	1.08580	0.0015
469.2	17000	1.07014	1.06755	0.0026
552.0	20000	1.05335	1.04989	0.0035
634.8	23000	1.03684	1.03273	0.0041
717.6	26000	1.02053	1.01597	0.0046
828.0	30000	0.99940	.99453	0.0049
938.4	34000	0.97880	.97354	0.0053
1048.8	38000	0.95867	.95323	0.0054
1159.2	42000	0.93906	.93357	0.0055
1269.6	46000	0.92001	.91465	0.0054
1380.0	50000	0.90159	.89643	0.0052
1490.4	54000	0.88397	.87898	0.0050
1600.8	58000	0.86711	.86230	0.0048
1711.2	62000	0.85107	.84638	0.0047
1821.6	66000	0.83586	.83126	0.0046
1932.0	70000	0.82146	.81693	0.0045
2042.4	74000	0.80785	.80337	0.0045

TABLE 2: 24 UO_2 - Er_2O_3 Rod MOX Assembly "High Enrichment" k_∞ Comparisons

Time (days)	Exposure (MWd/MT)	DIT	HELIOS	DIT - HELIOS
0	0	1.24321	1.24715	-0.0039
1.4	50	1.22300	1.22484	-0.0018
13.8	500	1.21359	1.21738	-0.0038
27.6	1000	1.20710	1.21073	-0.0036
55.2	2000	1.19708	1.20023	-0.0031
82.8	3000	1.18884	1.19151	-0.0027
138.0	5000	1.17470	1.17645	-0.0017
193.2	7000	1.16181	1.16260	-0.0008
248.4	9000	1.14963	1.14961	0.0000
303.6	11000	1.13794	1.13724	0.0007
386.4	14000	1.12131	1.11976	0.0015
469.2	17000	1.10531	1.10288	0.0024
552.0	20000	1.08973	1.08656	0.0032
634.8	23000	1.07449	1.07069	0.0038
717.6	26000	1.05944	1.05517	0.0043
828.0	30000	1.03989	1.03520	0.0047
938.4	34000	1.02057	1.01556	0.0050
1048.8	38000	1.00162	.99640	0.0052
1159.2	42000	0.98296	.97772	0.0052
1269.6	46000	0.96465	.95953	0.0051
1380.0	50000	0.94673	.94183	0.0049
1490.4	54000	0.92928	.92462	0.0047
1600.8	58000	0.91239	.90795	0.0044
1711.2	62000	0.89607	.89179	0.0043
1821.6	66000	0.88032	.87615	0.0042
1932.0	70000	0.86519	.86108	0.0041
2042.4	74000	0.85066	.84656	0.0041

TABLE 3: 48 UO_2 - Er_2O_3 Rod MOX Assembly "Low Enrichment" k_∞ Comparisons

Time (days)	Exposure (MWd/MT)	DIT	HELIOS	DIT - HELIOS
0	0	1.17957	1.18120	-0.0016
1.4	50	1.15686	1.15689	-0.0000
13.8	500	1.14783	1.14994	-0.0021
27.6	1000	1.14234	1.14451	-0.0022
55.2	2000	1.13476	1.13682	-0.0021
82.8	3000	1.12867	1.13062	-0.0019
138.0	5000	1.11799	1.11965	-0.0017
193.2	7000	1.10787	1.10911	-0.0012
248.4	9000	1.09797	1.09880	-0.0008
303.6	11000	1.08815	1.08856	-0.0004
386.4	14000	1.07373	1.07342	0.0003
469.2	17000	1.05912	1.05784	0.0013
552.0	20000	1.04412	1.04200	0.0021
634.8	23000	1.02881	1.02599	0.0028
717.6	26000	1.01321	1.00987	0.0033
828.0	30000	0.99256	.98875	0.0038
938.4	34000	0.97202	.96767	0.0043
1048.8	38000	0.95170	.94702	0.0047
1159.2	42000	0.93175	.92693	0.0048
1269.6	46000	0.91230	.90753	0.0048
1380.0	50000	0.89350	.88883	0.0047
1490.4	54000	0.87552	.87094	0.0046
1600.8	58000	0.85835	.85388	0.0045
1711.2	62000	0.84206	.83766	0.0044
1821.6	66000	0.82666	.82231	0.0043
1932.0	70000	0.81212	.80784	0.0043
2042.4	74000	0.79847	.79424	0.0042

TABLE 4: 48 UO_2 - Er_2O_3 Rod MOX Assembly "High Enrichment" k_∞ Comparisons

Time (days)	Exposure (MWd/MT)	DIT	HELIOS	DIT - HELIOS
0	0	1.20737	1.20896	-0.0016
1.4	50	1.18672	1.18685	-0.0001
13.8	500	1.17861	1.18058	-0.0020
27.6	1000	1.17348	1.17546	-0.0020
55.2	2000	1.16611	1.16791	-0.0018
82.8	3000	1.16024	1.16186	-0.0016
138.0	5000	1.15012	1.15139	-0.0013
193.2	7000	1.14063	1.14148	-0.0009
248.4	9000	1.13137	1.13186	-0.0005
303.6	11000	1.12220	1.12237	-0.0002
386.4	14000	1.10873	1.10837	0.0004
469.2	17000	1.09526	1.09413	0.0011
552.0	20000	1.08156	1.07972	0.0018
634.8	23000	1.06763	1.06516	0.0025
717.6	26000	1.05345	1.05047	0.0030
828.0	30000	1.03452	1.03105	0.0035
938.4	34000	1.01542	1.01150	0.0039
1048.8	38000	0.99637	.99214	0.0042
1159.2	42000	0.97744	.97305	0.0044
1269.6	46000	0.95874	.95436	0.0044
1380.0	50000	0.94039	.93609	0.0043
1490.4	54000	0.92247	.91829	0.0042
1600.8	58000	0.90510	.90105	0.0040
1711.2	62000	0.88831	.88433	0.0040
1821.6	66000	0.87214	.86819	0.0040
1932.0	70000	0.85660	.85268	0.0039
2042.4	74000	0.84172	.83776	0.0040

TABLE 5: 56 UO_2 - Er_2O_3 Rod MOX Assembly "Low Enrichment" k_∞ Comparisons

Time (days)	Exposure (MWd/MT)	DIT	HELIOS	DIT - HELIOS
0	0	1.16712	1.16796	-0.0008
1.4	50	1.14434	1.14367	0.0007
13.8	500	1.13566	1.13710	-0.0014
27.6	1000	1.13060	1.13215	-0.0015
55.2	2000	1.12382	1.12538	-0.0016
82.8	3000	1.11843	1.11998	-0.0015
138.0	5000	1.10892	1.11039	-0.0015
193.2	7000	1.09978	1.10104	-0.0013
248.4	9000	1.09073	1.09173	-0.0010
303.6	11000	1.08165	1.08234	-0.0007
386.4	14000	1.06814	1.06819	-0.0000
469.2	17000	1.05423	1.05336	0.0009
552.0	20000	1.03974	1.03803	0.0017
634.8	23000	1.02476	1.02234	0.0024
717.6	26000	1.00938	1.00642	0.0030
828.0	30000	0.98887	.98540	0.0035
938.4	34000	0.96838	.96431	0.0041
1048.8	38000	0.94803	.94358	0.0045
1159.2	42000	0.92801	.92338	0.0046
1269.6	46000	0.90848	.90385	0.0046
1380.0	50000	0.88960	.88506	0.0045
1490.4	54000	0.87156	.86709	0.0045
1600.8	58000	0.85435	.84995	0.0044
1711.2	62000	0.83804	.83368	0.0044
1821.6	66000	0.82264	.81833	0.0043
1932.0	70000	0.80814	.80389	0.0042
2042.4	74000	0.79454	.79034	0.0042

TABLE 6: 56 UO_2 - Er_2O_3 Rod MOX Assembly "High Enrichment" k_∞ Comparisons

Time (days)	Exposure (MWd/MT)	DIT	HELIOS	DIT - HELIOS
0	0	1.19659	1.19740	-0.0008
1.4	50	1.17593	1.17509	0.0008
13.8	500	1.16797	1.16926	-0.0013
27.6	1000	1.16317	1.16453	-0.0014
55.2	2000	1.15646	1.15775	-0.0013
82.8	3000	1.15118	1.15239	-0.0012
138.0	5000	1.14207	1.14311	-0.0010
193.2	7000	1.13341	1.13423	-0.0008
248.4	9000	1.12488	1.12549	-0.0006
303.6	11000	1.11636	1.11675	-0.0004
386.4	14000	1.10370	1.10370	0.0000
469.2	17000	1.09090	1.09018	0.0007
552.0	20000	1.07772	1.07630	0.0014
634.8	23000	1.06416	1.06211	0.0020
717.6	26000	1.05023	1.04766	0.0026
828.0	30000	1.03149	1.02839	0.0031
938.4	34000	1.01246	1.00888	0.0036
1048.8	38000	0.99340	.98947	0.0039
1159.2	42000	0.97440	.97027	0.0041
1269.6	46000	0.95560	.95144	0.0042
1380.0	50000	0.93713	.93301	0.0041
1490.4	54000	0.91910	.91506	0.0040
1600.8	58000	0.90162	.89765	0.0040
1711.2	62000	0.88472	.88081	0.0039
1821.6	66000	0.86846	.86453	0.0039
1932.0	70000	0.85285	.84891	0.0039

TABLE 7: 60 UO_2 - Er_2O_3 Rod MOX Assembly "Low Enrichment" k_∞ Comparisons

Time (days)	Exposure (MWd/MT)	DIT	HELIOS	DIT - HELIOS
0	0	1.15650	1.15726	-0.0008
1.4	50	1.13332	1.13260	0.0007
13.8	500	1.12465	1.12603	-0.0014
27.6	1000	1.11972	1.12122	-0.0015
55.2	2000	1.11326	1.11480	-0.0015
82.8	3000	1.10814	1.10970	-0.0016
138.0	5000	1.09903	1.10059	-0.0016
193.2	7000	1.09022	1.09159	-0.0014
248.4	9000	1.08143	1.08257	-0.0011
303.6	11000	1.07255	1.07339	-0.0008
386.4	14000	1.05924	1.05945	-0.0002
469.2	17000	1.04541	1.04467	0.0007
552.0	20000	1.03089	1.02929	0.0016
634.8	23000	1.01581	1.01347	0.0023
717.6	26000	1.00029	.99738	0.0029
828.0	30000	0.97959	.97614	0.0034
938.4	34000	0.95889	.95481	0.0041
1048.8	38000	0.93835	.93391	0.0044
1159.2	42000	0.91820	.91359	0.0046
1269.6	46000	0.89860	.89400	0.0046
1380.0	50000	0.87975	.87523	0.0045
1490.4	54000	0.86180	.85735	0.0045
1600.8	58000	0.84474	.84039	0.0044
1711.2	62000	0.82865	.82435	0.0043
1821.6	66000	0.81351	.80929	0.0042
1932.0	70000	0.79932	.79519	0.0041
2042.4	74000	0.78608	.78204	0.0040

TABLE 8: 60 UO_2 - Er_2O_3 Rod MOX Assembly "High Enrichment" k_∞ Comparisons

Time (days)	Exposure (MWd/MT)	DIT	HELIOS	DIT - HELIOS
0	0	1.18790	1.18867	-0.0008
1.4	50	1.16684	1.16597	0.0009
13.8	500	1.15887	1.16014	-0.0013
27.6	1000	1.15417	1.15551	-0.0013
55.2	2000	1.14770	1.14902	-0.0013
82.8	3000	1.14265	1.14392	-0.0013
138.0	5000	1.13389	1.13506	-0.0012
193.2	7000	1.12551	1.12651	-0.0010
248.4	9000	1.11722	1.11803	-0.0008
303.6	11000	1.10891	1.10951	-0.0006
386.4	14000	1.09649	1.09668	-0.0002
469.2	17000	1.08383	1.08328	0.0006
552.0	20000	1.07069	1.06943	0.0013
634.8	23000	1.05710	1.05518	0.0019
717.6	26000	1.04306	1.04063	0.0024
828.0	30000	1.02414	1.02117	0.0030
938.4	34000	1.00492	1.00142	0.0035
1048.8	38000	0.98565	.98176	0.0039
1159.2	42000	0.96644	.96234	0.0041
1269.6	46000	0.94746	.94329	0.0042
1380.0	50000	0.92883	.92468	0.0042
1490.4	54000	0.91069	.90660	0.0041
1600.8	58000	0.89314	.88910	0.0040
1711.2	62000	0.87621	.87220	0.0040
1821.6	66000	0.85997	.85594	0.0040
1932.0	70000	0.84442	.84037	0.0040
2042.4	74000	0.82957	.82548	0.0041

TABLE 9: 72 UO_2 - Er_2O_3 Rod MOX Assembly "Low Enrichment" k_∞ Comparisons

Time (days)	Exposure (MWd/MT)	DIT	HELIOS	DIT - HELIOS
0	0	1.13100	1.13112	-0.0001
1.4	50	1.10716	1.10592	0.0012
13.8	500	1.09873	1.09957	-0.0008
27.6	1000	1.09429	1.09533	-0.0010
55.2	2000	1.08888	1.09010	-0.0012
82.8	3000	1.08463	1.08602	-0.0014
138.0	5000	1.07694	1.07858	-0.0016
193.2	7000	1.06932	1.07096	-0.0016
248.4	9000	1.06152	1.06306	-0.0015
303.6	11000	1.05344	1.05477	-0.0013
386.4	14000	1.04110	1.04181	-0.0007
469.2	17000	1.02783	1.02757	0.0003
552.0	20000	1.01357	1.01242	0.0011
634.8	23000	0.99854	.99659	0.0020
717.6	26000	0.98290	.98034	0.0026
828.0	30000	0.96198	.95877	0.0032
938.4	34000	0.94098	.93708	0.0039
1048.8	38000	0.92014	.91583	0.0043
1159.2	42000	0.89976	.89529	0.0045
1269.6	46000	0.88003	.87557	0.0045
1380.0	50000	0.86123	.85682	0.0044
1490.4	54000	0.84343	.83910	0.0043
1600.8	58000	0.82665	.82241	0.0042
1711.2	62000	0.81096	.80681	0.0041
1821.6	66000	0.79633	.79231	0.0040
1932.0	70000	0.78275	.77887	0.0039
2042.4	74000	0.77022	.76653	0.0037

TABLE 10: 72 UO_2 - Er_2O_3 Rod MOX Assembly "High Enrichment" k_∞ Comparisons

Time (days)	Exposure (MWd/MT)	DIT	HELIOS	DIT - HELIOS
0	0	1.16678	1.16699	-0.0002
1.4	50	1.14497	1.14363	0.0013
13.8	500	1.13717	1.13800	-0.0008
27.6	1000	1.13282	1.13379	-0.0010
55.2	2000	1.12719	1.12826	-0.0011
82.8	3000	1.12288	1.12404	-0.0012
138.0	5000	1.11533	1.11663	-0.0013
193.2	7000	1.10798	1.10928	-0.0013
248.4	9000	1.10057	1.10182	-0.0012
303.6	11000	1.09301	1.09414	-0.0011
386.4	14000	1.08149	1.08229	-0.0008
469.2	17000	1.06947	1.06954	-0.0001
552.0	20000	1.05675	1.05607	0.0007
634.8	23000	1.04332	1.04196	0.0014
717.6	26000	1.02928	1.02739	0.0019
828.0	30000	1.01019	1.00770	0.0025
938.4	34000	0.99071	.98759	0.0031
1048.8	38000	0.97109	.96747	0.0036
1159.2	42000	0.95150	.94760	0.0039
1269.6	46000	0.93214	.92811	0.0040
1380.0	50000	0.91319	.90912	0.0041
1490.4	54000	0.89481	.89072	0.0041
1600.8	58000	0.87710	.87297	0.0041
1711.2	62000	0.86008	.85593	0.0041
1821.6	66000	0.84383	.83963	0.0042
1932.0	70000	0.82835	.82410	0.0042
2042.4	74000	0.81365	.80936	0.0043

0.000							
0.000							
W/H							
0.701	0.642						
0.703	0.643						
-0.002	-0.001						
1.095*	1.094	1.065					
1.094	1.100	1.090					
0.001	-0.006	-0.025					
1.000	1.059	1.041	0.000				
0.980	1.052	1.050	0.000				
0.020	0.007	-0.009	W/H				
0.975	1.044	1.035	0.000	0.000			
0.956	1.035	1.043	0.000	0.000			
0.019	0.009	-0.008	W/H	W/H			
0.968	1.022	1.084	1.041	1.047	1.064		
0.959	1.015	1.101*	1.048	1.053	1.079		
0.009	0.007	-0.017	-0.007	-0.006	-0.015		
0.992	0.552	1.045	1.073	1.081	1.076	0.585	
0.978	0.546	1.036	1.062	1.069	1.065	0.579	
0.014	0.006	0.009	0.011	0.012	0.011	0.006	
1.012	1.036	1.035	1.046	1.054	1.069	1.043	0.998
1.028	1.044	1.046	1.048	1.056	1.081	1.047	1.017
-0.016	-0.008	-0.011	-0.002	-0.002	-0.012	-0.004	-0.019

DIT
HELIOS
DIT-HELIOS

W/H denotes a water hole
* denotes the relative peak pin power

FIGURE 1. 24 UO_2 - Er_2O_3 Rod MOX Assembly "Low Enrichment" BOL Rel. Pin Power Dist.

0.000							
0.000							
W/H							
0.759	0.687						
0.759	0.690						
0.000	-0.003						
1.081	1.076	1.061					
1.080	1.081	1.088					
0.001	-0.005	-0.027					
0.985	1.039	1.082	0.000				
0.964	1.029	1.093	0.000				
0.021	0.010	-0.011	W/H				
0.962	1.024	1.077	0.000	0.000			
0.941	1.014	1.087	0.000	0.000			
0.021	0.010	-0.010	W/H	W/H			
0.956	1.006	1.072	1.083	1.089*	1.059		
0.946	0.998	1.090	1.092	1.097*	1.075		
0.010	0.008	-0.018	-0.009	-0.008	-0.016		
0.981	0.589	1.030	1.053	1.060	1.056	0.622	
0.967	0.584	1.019	1.040	1.046	1.043	0.614	
0.014	0.005	0.011	0.013	0.014	0.013	0.008	
1.003	1.026	1.024	1.033	1.040	1.053	1.040	1.014
1.021	1.035	1.036	1.035	1.042	1.065	1.045	1.038
-0.018	-0.009	-0.012	-0.002	-0.002	-0.012	-0.005	-0.024

DIT
HELIOS
DIT-HELIOS

W/H denotes a water hole
* denotes the relative peak pin power

FIGURE 2. 24 UO_2 - Er_2O_3 Rod MOX Assembly "High Enrichment" BOL Rel. Pin Power Dist.

0.000							
0.000							
W/H							
0.721	1.062						
0.722	1.076						
-0.001	-0.014						
1.107	1.095	0.695					
1.104	1.106	0.700					
0.003	-0.011	-0.005					
1.060	1.088	0.774	0.000				
1.040	1.088	0.775	0.000				
0.020	0.000	-0.001	W/H				
1.025	1.100	0.760	0.000	0.000			
1.004	1.097	0.762	0.000	0.000			
0.021	0.003	-0.002	W/H	W/H			
0.997	1.064	1.058	0.766	0.781	0.697		
0.983	1.065	1.064	0.767	0.780	0.698		
0.014	-0.001	-0.006	-0.001	0.001	-0.001		
0.994	1.023	1.092	1.096	1.074	1.087	1.096	
0.983	1.018	1.091	1.090	1.069	1.083	1.094	
0.011	0.005	0.001	0.006	0.005	0.004	0.002	
1.027	1.041	1.070	1.109*	1.091	1.096	1.036	0.994
1.040	1.053	1.078	1.110*	1.092	1.104	1.045	1.008
-0.013	-0.012	-0.008	-0.001	-0.001	-0.008	-0.009	-0.014

DIT
HELIOS
DIT-HELIOS

W/H denotes a water hole
* denotes the relative peak pin power

FIGURE 3. 48 UO_2 - Er_2O_3 Rod MOX Assembly "Low Enrichment" BOL Rel. Pin Power Dist.

0.000							
0.000							
W/H							
0.769	1.079						
0.770	1.095						
-0.001	-0.016						
1.090*	1.085	0.738					
1.085	1.096*	0.743					
0.005	-0.011	-0.005					
1.035	1.082	0.829	0.000				
1.013	1.081	0.831	0.000				
0.022	0.001	-0.002	W/H				
1.004	1.086	0.813	0.000	0.000			
0.981	1.083	0.817	0.000	0.000			
0.023	0.003	-0.004	W/H	W/H			
0.978	1.041	1.079	0.819	0.835	0.739		
0.963	1.041	1.088	0.822	0.837	0.742		
0.015	0.000	-0.009	-0.003	-0.002	-0.003		
0.977	1.003	1.068	1.089	1.076	1.075	1.071	
0.965	0.996	1.066	1.083	1.071	1.071	1.067	
0.012	0.007	0.002	0.006	0.005	0.004	0.004	
1.012	1.024	1.050	1.085	1.072	1.074	1.029	1.010
1.025	1.037	1.059	1.086	1.073	1.082	1.040	1.030
-0.013	-0.013	-0.009	-0.001	-0.001	-0.008	-0.011	-0.020

DIT
HELIOS
DIT-HELIOS

W/H denotes a water hole
* denotes the relative peak pin power

FIGURE 4. 48 UO_2 - Er_2O_3 Rod MOX Assembly "High Enrichment" BOL Rel. Pin Power Dist.

0.000							
0.000							
W/H							
0.738	1.037						
0.739	1.051						
-0.001	-0.014						
1.095	1.082	0.713					
1.092	1.092	0.717					
0.003	-0.010	-0.004					
1.088	1.072	0.793	0.000				
1.069	1.073	0.793	0.000				
0.019	-0.001	0.000	W/H				
1.049	1.092	0.786	0.000	0.000			
1.028	1.091	0.786	0.000	0.000			
0.021	0.001	0.000	W/H	W/H			
1.017	1.110	0.691	0.791	0.795	0.707		
1.002	1.110	0.692	0.791	0.795	0.707		
0.015	0.000	-0.001	0.000	0.000	0.000		
1.010	1.050	1.102	1.082	1.093	1.097	1.097	
0.999	1.051	1.099	1.078	1.089	1.093	1.095	
0.011	-0.001	0.003	0.004	0.004	0.004	0.002	
1.040	1.058	1.096	1.095	1.108*	1.102	1.075	1.033
1.053	1.072	1.103	1.096	1.109*	1.109	1.086	1.050
-0.013	-0.014	-0.007	-0.001	-0.001	-0.007	-0.011	-0.017

DIT
HELIOS
DIT-HELIOS

W/H denotes a water hole
* denotes the relative peak pin power

FIGURE 5. 56 UO_2 - Er_2O_3 Rod MOX Assembly "Low Enrichment" BOL Rel. Pin Power Dist.

0.000							
0.000							
W/H							
0.783	1.062						
0.785	1.078						
-0.002	-0.016						
1.080	1.076	0.751					
1.076	1.086	0.758					
0.004	-0.010	-0.007					
1.057	1.071	0.846	0.000				
1.035	1.071	0.848	0.000				
0.022	0.000	-0.002	W/H				
1.023	1.024	0.840	0.000	0.000			
1.000	1.083	0.842	0.000	0.000			
0.023	-0.059	-0.002	W/H	W/H			
0.995	1.086	0.733	0.845	0.849	0.748		
0.979	1.085	0.737	0.846	0.850	0.750		
0.016	0.001	-0.004	-0.001	-0.001	-0.002		
0.991	1.028	1.085	1.084	1.093*	1.084	1.072	
0.979	1.028	1.081	1.079	1.088*	1.079	1.068	
0.012	0.000	0.004	0.005	0.005	0.005	0.004	
1.023	1.039	1.072	1.075	1.086	1.079	1.059	1.039
1.036	1.052	1.079	1.076	1.087	1.086	1.071	1.061
-0.013	-0.013	-0.007	-0.001	-0.001	-0.007	-0.012	-0.022

DIT
HELIOS
DIT-HELIOS

W/H denotes a water hole
* denotes the relative peak pin power

FIGURE 6. 56 UO_2 - Er_2O_3 Rod MOX Assembly "High Enrichment" BOL Rel. Pin Power Dist.

0.000							DIT	
0.000							HELIOS	
W/H							DIT-HELIOS	
0.747	1.050							
0.748	1.064							
-0.001	-0.014						W/H denotes a water hole	
							* denotes the relative peak pin power	
1.109*	1.096	0.723						
1.106*	1.106	0.727						
0.003	-0.010	-0.004						
1.104	1.090	0.805	0.000					
1.085	1.090	0.806	0.000					
0.019	0.000	-0.001	W/H					
1.068	1.067	0.800	0.000	0.000				
1.047	1.067	0.801	0.000	0.000				
0.021	0.000	-0.001	W/H	W/H				
1.036	1.096	0.706	0.810	0.820	0.740			
1.022	1.095	0.708	0.810	0.819	0.741			
0.014	0.001	-0.002	0.000	0.001	-0.001			
1.028	1.074	1.091	1.071	1.095	1.084	0.668		
1.017	1.074	1.088	1.067	1.090	1.078	0.664		
0.011	0.000	0.003	0.004	0.005	0.006	0.004		
1.057	1.081	1.092	1.100	1.081	1.094	1.078	1.058	
1.070	1.096	1.099	1.102	1.083	1.105	1.085	1.080	
-0.013	-0.015	-0.007	-0.002	-0.002	-0.011	-0.007	-0.022	

FIGURE 7. 60 UO_2 - Er_2O_3 Rod MOX Assembly "Low Enrichment" BOL Rel. Pin Power Dist.

0.000							DIT	
0.000							HELIOS	
W/H							DIT-HELIOS	
0.790	1.073							
0.792	1.088							
-0.002	-0.015						W/H denotes a water hole	
							* denotes the relative peak pin power	
1.091	1.087	0.762						
1.086	1.097*	0.766						
0.005	-0.010	-0.004						
1.069	1.085	0.856	0.000					
1.047	1.085	0.858	0.000					
0.022	0.000	-0.002	W/H					
1.037	1.065	0.852	0.000	0.000				
1.014	1.064	0.853	0.000	0.000				
0.023	0.001	-0.001	W/H	W/H				
1.009	1.074	0.746	0.861	0.869	0.776			
0.993	1.073	0.749	0.862	0.870	0.778			
0.016	0.001	-0.003	-0.001	-0.001	-0.002			
1.003	1.046	1.076	1.076	1.096*	1.082	0.692		
0.991	1.045	1.072	1.072	1.091	1.075	0.688		
0.012	0.001	0.004	0.004	0.005	0.007	0.004		
1.035	1.056	1.068	1.078	1.065	1.075	1.071	1.063	
1.049	1.070	1.076	1.080	1.067	1.086	1.078	1.090	
-0.014	-0.014	-0.008	-0.002	-0.002	-0.011	-0.007	-0.027	

FIGURE 8. 60 UO_2 - Er_2O_3 Rod MOX Assembly "High Enrichment" BOL Rel. Pin Power Dist.

0.000								
0.000								
W/H								
0.801	0.747							
0.800	0.750							
0.001	-0.003							
1.095	1.078	0.766						
1.094	1.085	0.770						
0.001	-0.007	-0.004						
1.098	1.107	0.843	0.000					
1.081	1.106	0.844	0.000					
0.017	0.001	-0.001	W/H					
1.097	1.081	0.838	0.000	0.000				
1.077	1.079	0.838	0.000	0.000				
0.020	0.002	0.000	W/H	W/H				
1.110	1.097	0.748	0.849	0.856	0.775			
1.101	1.092	0.751	0.849	0.856	0.776			
0.009	0.005	-0.003	0.000	0.000	-0.001			
1.085	0.639	1.091	1.084	1.100	1.087	0.704		
1.073	0.636	1.084	1.080	1.096	1.081	0.700		
0.012	0.003	0.007	0.004	0.004	0.006	0.004		
1.102	1.108	1.097	1.082	1.099	1.108*	1.083	1.084	
1.123	1.118	1.107	1.085	1.103	1.119*	1.090	1.108	
-0.021	-0.010	-0.010	-0.003	-0.004	-0.011	-0.007	-0.024	

DIT
HELIOS
DIT-HELIOS

W/H denotes a water hole
* denotes the relative peak pin power

FIGURE 9. 72 UO_2 - Er_2O_3 Rod MOX Assembly "Low Enrichment" BOL Rel. Pin Power Dist.

0.000								
0.000								
W/H								
0.840	0.776							
0.840	0.782							
0.000	-0.006							
1.087	1.086	0.798						
1.085	1.093	0.804						
0.002	-0.007	-0.006						
1.064	1.101*	0.887	0.000					
1.044	1.099	0.889	0.000					
0.020	0.002	-0.002	W/H					
1.058	1.078	0.882	0.000	0.000				
1.036	1.075	0.884	0.000	0.000				
0.022	0.003	-0.002	W/H	W/H				
1.067	1.081	0.781	0.892	0.898	0.803			
1.055	1.077	0.785	0.893	0.898	0.806			
0.012	0.004	-0.004	-0.001	0.000	-0.003			
1.053	0.664	1.083	1.089	1.101	1.085	0.720		
1.039	0.661	1.076	1.084	1.096	1.078	0.715		
0.014	0.003	0.007	0.005	0.005	0.007	0.005		
1.071	1.082	1.074	1.066	1.080	1.086	1.075	1.084	
1.092	1.093	1.085	1.069	1.083	1.097	1.083	1.112*	
-0.021	-0.011	-0.011	-0.003	-0.003	-0.011	-0.008	-0.028	

DIT
HELIOS
DIT-HELIOS

W/H denotes a water hole
* denotes the relative peak pin power

FIGURE 10. 72 UO_2 - Er_2O_3 Rod MOX Assembly "High Enrichment" BOL Rel. Pin Power Dist.

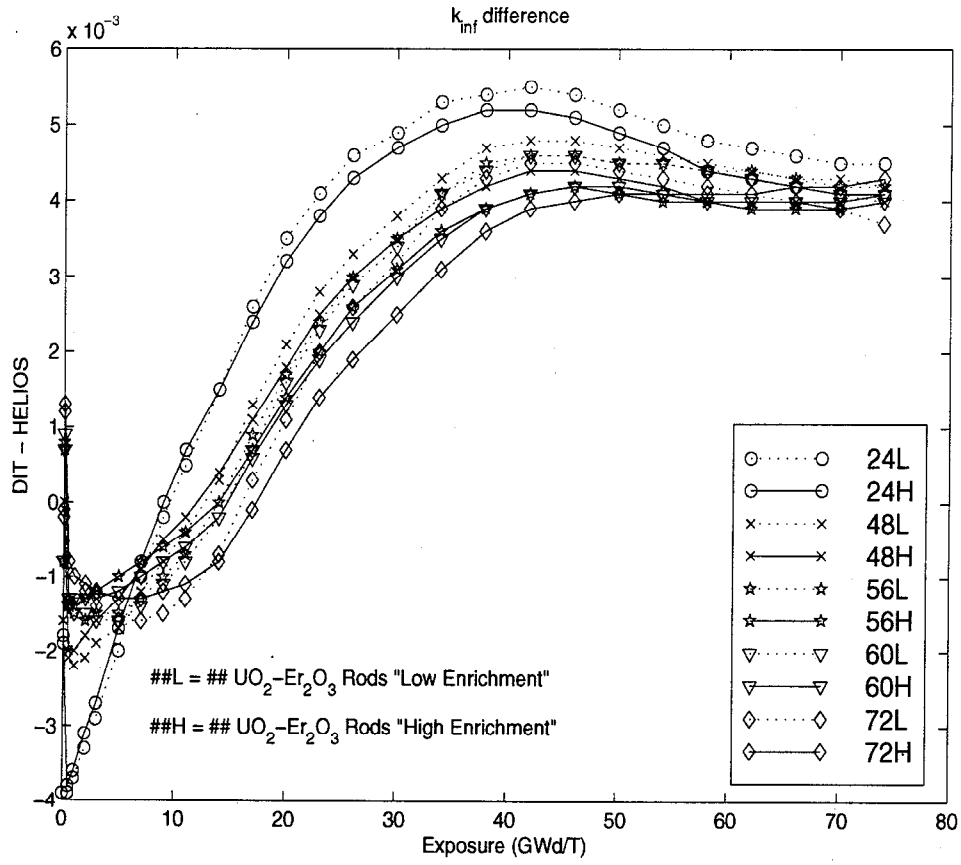

FIGURE 11. k_{inf} Differences for Various ABB-CE MOX Lattices

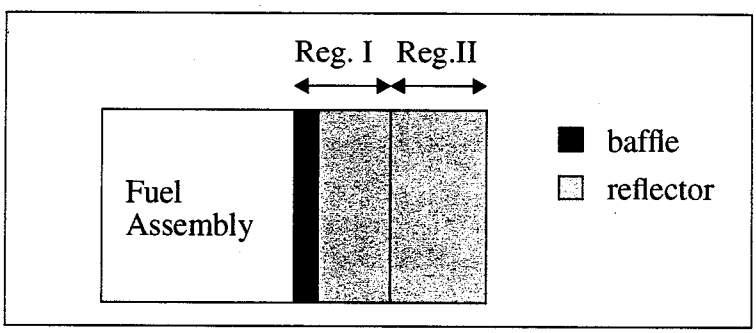

TABLE 11: Baffle/Reflector ADFs for Various MOX Lattices and LEU Lattice

MOX Lattice	Region I		Region II	
	ADF_1	ADF_2	ADF_1	ADF_2
24 Low	9.7489E-01	1.8475E-01	5.1612E-01	3.5025E-01
24 High	9.6921E-01	1.7484E-01	5.1366E-01	3.4776E-01

TABLE 11: Baffle/Reflector ADFs for Various MOX Lattices and LEU Lattice

MOX Lattice	Region I		Region II	
	ADF_1	ADF_2	ADF_1	ADF_2
48 Low	9.8136E-01	1.8794E-01	5.2169E-01	3.5419E-01
48 High	9.7486E-01	1.7729E-01	5.1857E-01	3.5120E-01
56 Low	9.8319E-01	1.8839E-01	5.2347E-01	3.5537E-01
56 High	9.7644E-01	1.7770E-01	5.2012E-01	3.5225E-01
60 Low	9.8554E-01	1.9341E-01	5.2428E-01	3.5636E-01
60 High	9.7832E-01	1.8148E-01	5.2075E-01	3.5300E-01
72 Low	9.9051E-01	1.9964E-01	5.2754E-01	3.5899E-01
72 High	9.8245E-01	1.8618E-01	5.2346E-01	3.5523E-01
LEU	9.9797E-01	2.9217E-01	5.2484E-01	3.6333E-01

TABLE 12: Baffle/Reflector Diffusion Coefficients for Various MOX Lattices and LEU Lattice

MOX Lattice	Region I		Region II	
	D_1	D_2	D_1	D_2
24 Low	1.0628E+00	2.9252E-01	1.5654E+00	2.7810E-01
24 High	1.0651E+00	2.9226E-01	1.5661E+00	2.7809E-01
48 Low	1.0647E+00	2.9211E-01	1.5663E+00	2.7770E-01
48 High	1.0666E+00	2.9197E-01	1.5666E+00	2.7780E-01
56 Low	1.0654E+00	2.9200E-01	1.5666E+00	2.7761E-01
56 High	1.0671E+00	2.9190E-01	1.5667E+00	2.7774E-01
60 Low	1.0643E+00	2.9205E-01	1.5665E+00	2.7754E-01
60 High	1.0661E+00	2.9197E-01	1.5665E+00	2.7772E-01
72 Low	1.0642E+00	2.9196E-01	1.5670E+00	2.7734E-01
72 High	1.0659E+00	2.9196E-01	1.5665E+00	2.7763E-01
LEU	1.0427E+00	2.9491E-01	1.5491E+00	2.7744E-01

4. HELIOS/FORMOSA-P versus DIT/ROCS Predictions for Full MOX Core

FORMOSA-P models have been established for the equilibrium cycle, full MOX cores identified by ABB-CE [1], contrasting predictions of core attributes with the ABB-CE core simulator ROCS predictions. An equilibrium cycle, full MOX core is established in FORMOSA-P in an iterative manner. Beginning-of-Cycle (BOC) assembly quadrant isotopics, associated with the 2x2 spatial radial mesh/assembly being employed, are initially estimated by assuming them uniform across the assembly, obtaining the isotopics from HELIOS utilizing the ROCS predicted assembly average burnups. This initialization

process ignores both the assembly quadrant-wise spatial dependence and core position dependent spectral history effects. In addition, equilibrium *Sm* conditions are assumed at BOC, in error since feed assemblies have no *Sm* and burned assemblies have peak Sm. These initialization approximations are necessary based upon the information available. The cycle is then depleted utilizing FORMOSA-P, and BOC reestablished based upon the End-of-Cycle (EOC) isotopics and appropriate *Sm* conditions predicted by FORMOSA-P. This process is repeated until BOC attributes converge. For each cycle, the ROCS predicted critical soluble boron values are employed, and FORMOSA-P completes a critical axial buckling search. This is necessary, since FORMOSA-P is a two-dimensional code. The implication is that contrasting ROCS and FORMOSA-P predicted critical soluble boron values is meaningless.

The equilibrium cycle, full MOX cores for all four cases determined by ABB-CE [1] have been established; however, at this point we will be focusing on CASE 2 (Figure 12), whose feed loading is indicated in Table 13. Figure 13 through Figure 15 show the BOC assembly burnup, assembly power and assembly k_∞ distributions, respectively. For BOC, equilibrium Xenon and peak Samarium (burnt assemblies)/no Samarium (feed assemblies) fission product conditions are used. BOC assembly burnups show very good agreement. Good agreement is also shown for the BOC assembly power map. Figure 16 through Figure 18 show the results at EOC. Again, very good agreement is observed. The core performance characteristics' comparisons are shown in Table 14. Overall, the agreement in predicted core attributes by DIT/ROCS versus HELIOS/FORMOSA-P is considered to be very good. The FORMOSA-P equilibrium cycle, full MOX core model for CASE 2 provides the starting point for the mixed LEU-MOX core study.

TABLE 13: CASE 2 Equilibrium Cycle, Full MOX Core Feed Batches

# Assem-blies	# of MOX Fuel Rods	w/o WG-Pu	# of UO_2-Er_2O_3 BP Rods	Er_2O_3 Loading (w/o)	w/o ^{235}U of BP Rods
25	212	6.00	24	2.1	5.50
56	180	4.71	56	2.1	4.30
81		5.16		2.1	4.49

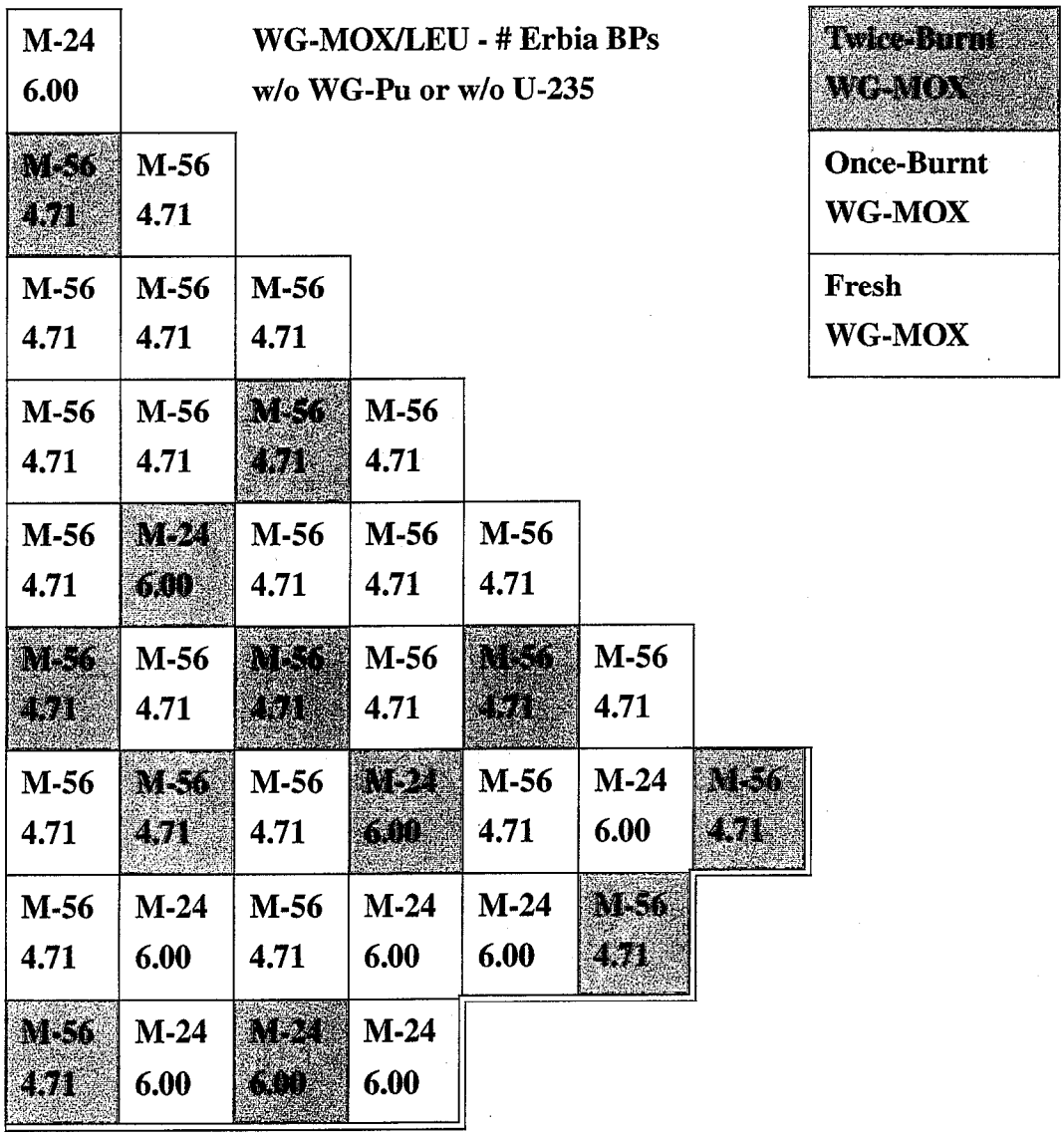

FIGURE 12. Equilibrium Cycle, Full MOX Core Loading Pattern

TABLE 14: CASE 2 Equilibrium Cycle, Full MOX Core Performance Characteristics Predictions for DIT/ROCS vs. HELIOS/FORMOSAP

	DIT/ROCS	HELIOS/F-P	Difference
F_r (HFP,BOC)	1.60	1.57	0.03
Boron Worth (pcm/PPM)			
HFP,BOC	-4.329	-3.753	-0.576 pcm/PPM
HFP,EOC	-5.848	-5.227	-0.621 pcm/PPM
MTC (pcm/^{o}F)			
HFP,BOC	-18.9	-22.1	-3.2 pcm/^{o}F
HFP,EOC	-38.8	-42.2	-3.4 pcm/^{o}F

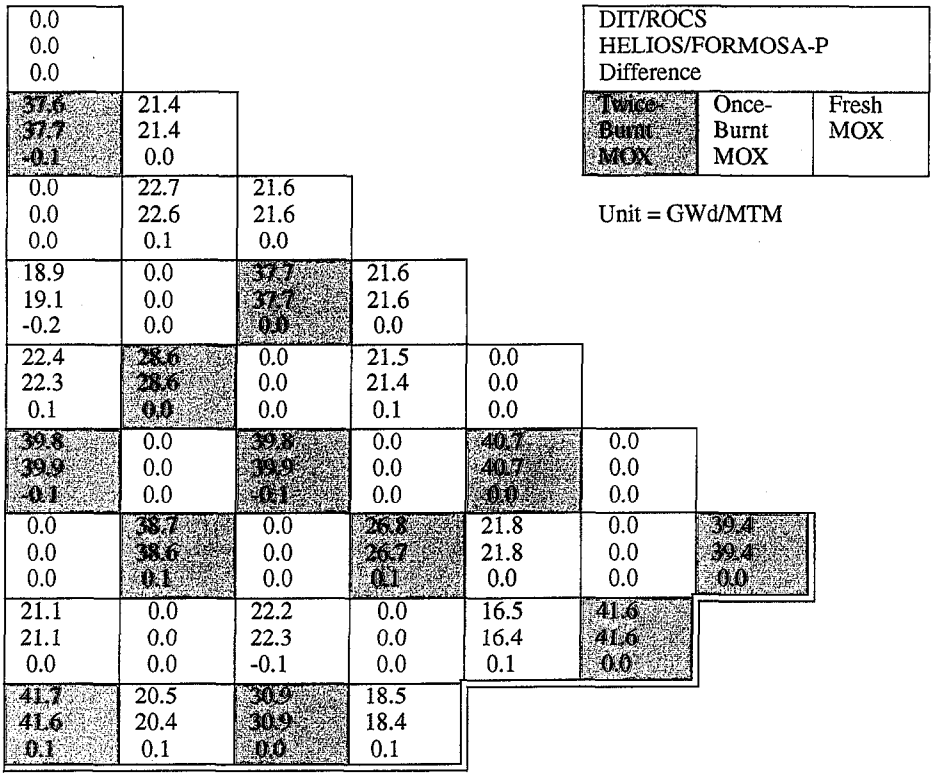

FIGURE 13. CASE 2: Equilibrium Cycle, Full MOX Core BOC Assembly Burnup Distribution

1.33 1.35 -0.02						
0.93 0.95 -0.02	1.05 1.06 -0.01					
1.35 1.34 0.01	1.12 1.12 0.00	1.04 1.05 -0.01				
1.28 1.26 0.02	1.37 1.36 0.01	0.95 0.96 -0.01	1.05 1.06 -0.01			
1.16 1.16 0.00	1.24 1.24 0.00	1.33 1.33 0.00	1.13 1.14 -0.01	1.25 1.25 0.00		
0.98 0.97 0.01	1.30 1.30 0.00	1.00 1.00 0.00	1.28 1.27 0.01	0.89 0.89 0.00	1.11 1.11 0.00	
1.26 1.26 0.00	0.98 0.99 -0.01	1.29 1.28 0.01	1.14 1.14 0.00	0.91 0.91 0.00	0.96 0.96 0.00	0.37 0.37 0.00
0.97 0.98 -0.01	1.25 1.25 0.00	0.98 0.97 0.01	1.12 1.12 0.00	0.69 0.69 0.00	0.30 0.30 0.00	
0.44 0.44 0.00	0.60 0.60 0.00	0.53 0.53 0.00	0.47 0.46 0.01			

DIT/ROCS HELIOS/FORMOSA-P Difference		
Twice-Burnt MOX	Once-Burnt MOX	Fresh MOX

FIGURE 14. CASE 2: Equilibrium Cycle, Full MOX Core BOC Assembly Power Distribution

1.18 1.19 -0.01						
0.91 0.91 0.00	1.00 1.00 0.00					
1.10 1.10 0.00	0.99 0.99 0.00	0.99 1.00 -0.01				
1.01 1.00 0.01	1.10 1.10 0.00	0.91 0.91 0.00	0.99 1.00 -0.01			
0.99 0.99 0.00	1.01 1.01 0.00	1.10 1.10 0.00	0.99 0.99 -0.01	1.11 1.10 0.01		
0.90 0.90 0.00	1.10 1.10 0.00	0.90 0.90 0.00	1.11 1.10 0.01	0.90 0.90 0.00	1.11 1.11 0.00	
1.11 1.10 0.01	1.11 1.10 0.01	0.91 0.91 0.00	1.10 1.10 0.00	1.02 1.02 0.00	1.19 1.20 -0.01	0.91 0.92 -0.01
1.00 1.00 0.00	1.18 1.19 -0.01	0.99 1.00 -0.01	1.19 1.19 0.00	1.09 1.09 0.00	0.91 0.91 0.00	
0.90 0.91 -0.01	1.07 1.07 0.00	1.01 1.02 -0.01	1.09 1.09 0.00			

DIT/ROCS HELIOS/FORMOSA-P Difference		
Twice-Burnt MOX	Once-Burnt MOX	Fresh MOX

FIGURE 15. CASE 2: Equilibrium Cycle, Full MOX Core BOC Assembly k_∞ Distribution

22.0 22.0 0.0						
53.7 53.8 -0.1	39.4 39.5 -0.1					
22.4 22.3 0.1	41.6 41.5 0.1	39.5 39.5 0.0				
39.8 39.9 -0.1	22.7 22.6 0.1	54.1 54.2 -0.1	39.8 39.9 -0.1			
41.7 41.6 0.1	49.0 49.2 -0.2	22.2 22.3 -0.1	40.7 40.7 0.0	21.4 21.4 0.0		
56.5 56.4 0.1	21.8 21.8 0.0	56.8 57.0 -0.2	21.6 21.6 0.0	56.3 56.3 0.0	19.2 19.1 0.1	
21.1 21.1 0.0	55.3 55.2 0.1	21.5 21.4 0.1	45.8 45.7 0.1	37.7 37.7 0.0	16.5 16.4 0.1	46.2 46.2 0.0
37.6 37.5 0.1	20.5 20.4 0.1	38.7 38.6 0.1	18.5 18.4 0.1	28.6 28.6 0.0	47.2 47.2 0.0	
49.7 49.6 0.1	30.9 30.9 0.0	40.4 40.2 0.2	26.8 26.7 0.1			

DIT/ROCS HELIOS/FORMOSA-P Difference		
Thrice-Burnt MOX	Twice-Burnt MOX	Once-Burnt MOX

FIGURE 16. CASE 2: Equilibrium Cycle, Full MOX Core EOC Assembly Burnup Distribution

1.25 1.24 0.01						
0.93 0.94 -0.01	1.03 1.04 -0.01					
1.27 1.26 0.01	1.07 1.08 -0.01	1.03 1.04 -0.01				
1.17 1.17 0.00	1.29 1.28 0.01	0.96 0.97 -0.01	1.06 1.06 0.00			
1.10 1.10 0.00	1.17 1.18 -0.01	1.28 1.28 0.00	1.12 1.12 0.00	1.27 1.26 0.01		
0.98 0.98 0.00	1.27 1.27 0.00	1.01 1.01 0.00	1.27 1.27 0.00	0.95 0.95 0.00	1.17 1.16 0.01	
1.25 1.24 0.01	0.99 0.99 0.00	1.26 1.26 0.00	1.12 1.12 0.00	0.96 0.96 0.00	1.01 1.00 0.01	0.44 0.45 -0.01
0.98 0.97 0.01	1.20 1.19 0.01	0.98 0.97 0.01	1.09 1.09 0.00	0.75 0.76 -0.01	0.37 0.38 -0.01	
0.50 0.51 -0.01	0.65 0.66 -0.01	0.59 0.59 0.00	0.51 0.53 -0.02			

DIT/ROCS HELIOS/FORMOSA-P Difference		
Thrice-Burnt MOX	Twice-Burnt MOX	Once-Burnt MOX

FIGURE 17. CASE 2: Equilibrium Cycle, Full MOX Core EOC Assembly Power Distribution

1.13 1.13 0.00						
0.94 0.94 0.00	1.00 1.00 0.00					
1.09 1.08 0.01	1.00 0.99 0.01	1.00 1.00 0.00				
1.00 1.00 0.00	1.09 1.08 0.01	0.94 0.94 0.00	1.00 1.00 0.00			
0.99 0.99 0.00	1.00 1.00 0.00	1.09 1.08 0.01	1.00 1.00 0.00	1.09 1.09 0.00		
0.93 0.93 0.00	1.09 1.09 0.00	0.93 0.92 0.01	1.09 1.09 0.00	0.93 0.93 0.00	1.11 1.10 0.01	
1.10 1.09 0.01	0.94 0.93 0.01	1.09 1.09 0.00	1.02 1.02 0.00	1.02 1.01 0.01	1.16 1.16 0.00	0.98 0.98 0.00
1.02 1.01 0.01	1.14 1.14 0.00	1.01 1.01 0.00	1.15 1.15 0.00	1.11 1.10 0.01	0.98 0.98 0.00	
0.97 0.96 0.01	1.10 1.10 0.00	1.05 1.05 0.00	1.13 1.12 0.01			

DIT/ROCS HELIOS/FORMOSA-P Difference		
Twice-Burnt MOX	Twice-Burnt MOX	Once-Burnt MOX

FIGURE 18. CASE 2: Equilibrium Cycle, Full MOX Core EOC Assembly k_∞ Distribution

5. Initial Mixed Core

Several scenarios were examined in regard to mixed LEU-MOX cores starting with the CASE 2 equilibrium cycle, full MOX core. All scenarios have in common that the first cycle that LEU feed assemblies are loaded into the core, all MOX feed assemblies are unavailable and replaced by LEU feed assemblies. This will be referred to as the Initial Mixed Core. In subsequent cycles, different scenarios are assumed depending upon the availability of MOX feed assemblies, as will be described in Section 6. For all scenarios, the LEU lattice designs used are the standard ABB-CE LEU lattice designs (Figure 19).

For the initial mixed LEU-MOX core, the following design approach was employed. First, the non-dominant (Table 13) MOX feed batch, *i.e.* smaller size feed batch, is replaced by an LEU feed batch to find the "equivalent" LEU feed batch whose BP loading and ^{235}U enrichment produce the same cycle energy production and maximum soluble boron concentration for the first cycle loaded, utilizing the minimum non-dominant batch feed enrichment possible. In completing this assessment of the lattice attributes of the non-dominant LEU feed batch, the core LP is fixed and dominant MOX feed batch retained, with the only constraints imposed being those noted above, *i.e.* cycle energy requirement and maximum soluble boron concentration. This assessment is completed utilizing FORMOSA-P without automatic optimization capability activated. Note that no burnable poison rods were found necessary for the non-dominant equivalent LEU feed batch to hold down the soluble boron concentration to an acceptable value.

Fixing the non-dominant LEU feed batch at the equivalent feed batch attributes, the dominant LEU feed batch is determined such that the cycle energy requirement and all constraints [maximum soluble boron concentration (2,000 ppm), radial pin-wise power peaking (1.60), and maximum pin-wise discharge burnup (60 GWd/MTHM)] are satisfied and the dominant LEU feed batch enrichment is minimized (Table 15). This is accomplished utilizing FORMOSA-P with the automatic optimization capability activated. In determining the optimum dominant LEU feed batch attributes, MOX burnt assemblies are allowed to shuffle while feed assemblies are fixed to their original locations. FORMOSA-P was rerun several times for different but fixed numbers of burnable poison rods in the dominant LEU feed batch. This approach is necessary, since we wish to employ only two LEU feed batch designs, as was done with the MOX feed

batch designs. Normally, FORMOSA-P would optimize by utilizing different numbers of burnable poison rods in the dominant LEU feed batch assemblies; hence, the need for the altered approach taken to limit the selection to the same number of burnable poison rods.

As noted in Figure 20 and Figure 21, with the objective being to minimize the enrichment of the dominant LEU feed batch enrichment, a very low leakage loading pattern results as to be expected. Table 16 summarizes the full MOX and initial LEU-MOX mixed cores' attributes. The maximum soluble boron concentration for the initial mixed LEU-MOX core is slightly lower than that for the CASE 2 full MOX core, well within the maximum limit of 2,000 ppm. The maximum radial pin-wise peaking factor is slightly higher for the initial mixed LEU-MOX core versus full MOX core, but within the imposed limit of 1.60. BOC and EOC assembly power distributions and assembly burnups are shown in Figure 21 and Figure 22, respectively. At both BOC and EOC, the maximum radial peaking factor occurs in a once-burnt MOX assembly adjacent to an LEU feed assembly. Apparently, thermal neutron diffusion from the LEU to MOX assembly, caused by the much softer energy spectrum in the LEU assembly, is causing the power peaking in the adjacent MOX assembly. The peak pin burnup (Figure 22) is noted to slightly exceed (0.2 GWd/MTHM) the limit of 60 GWd/MTHM, likely an acceptable result or correctable via further LP tuning. Finally, note that the average feed enrichment is 4.17 w/o ^{235}U. For an equilibrium, full LEU core with the same cycle energy requirement, the average feed enrichment is about 5.0 w/o ^{235}U. Why the mixed LEU-MOX core exhibits a lower average feed enrichment is because of more reactivity carry-forward in the once and twice burnt MOX assemblies. This can be seen in Figure 23, where we see that the rate of decrease of assembly reactivity with burnup is greater for LEU versus MOX assemblies.

The resulting LP for the initial mixed core is the starting point for the optimization of subsequent cycles as now explained.

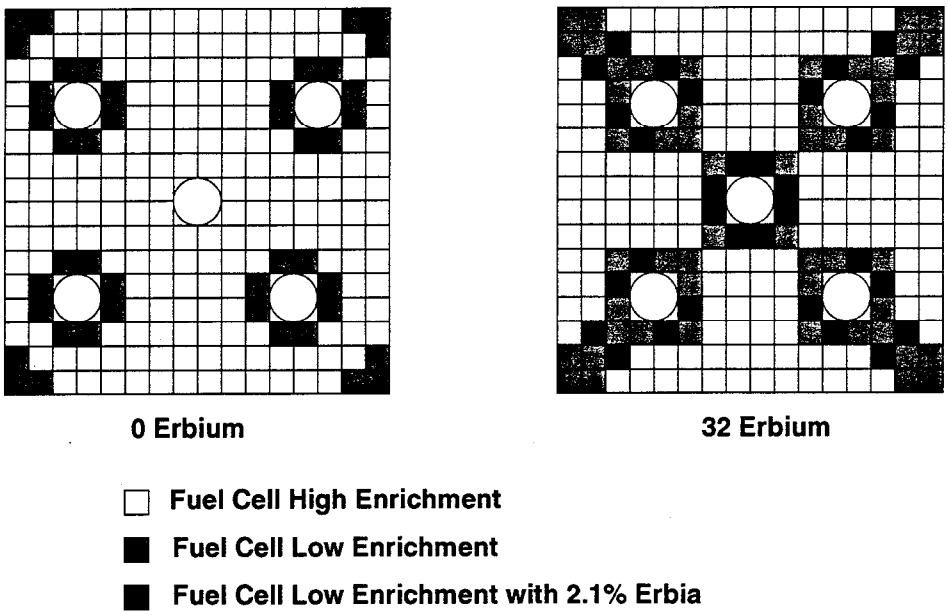

FIGURE 19. Example of ABB-CE Standard LEU Lattice Designs

TABLE 15: Initial Mixed Core Feed Batches

Feed Batch Composition	Equilibrium Cycle, Full MOX Core		Initial Mixed Core	
	25 Assemblies	56 Assemblies	25 Assemblies	56 Assemblies
# Er_2O_3-UO_2 Rods	24	56	0	48
Average Enrichment	6.00 wt% WGPu	4.71 wt% WGPu	4.74 wt% ^{235}U	3.91 wt% ^{235}U

TABLE 16: CASE 2 Full MOX & Initial Mixed Cores Performance Characteristics

Characteristic	Equilibrium Cycle, Full MOX	Initial Mixed Core
Maximum $F_{\Delta H}$	1.57	1.60
HFP, BOC Boron Worth	-3.75 pcm/ppm	-5.17 pcm/ppm
HFP, EOC Boron Worth	-5.23 pcm/ppm	-6.52 pcm/ppm
HFP, BOC MTC	-22.1 pcm/°F	-16.1 pcm/°F
HFP, EOC MTC	-42.2 pcm/°F	-30.2 pcm/°F
Maximum Soluble Boron	1928 ppm	1774 ppm
Maximum Pin Discharge Burnup	59,671 MWd/MTM	60,184 MWd/MTM

MOX or LEU - # Erbia BPs
w/o WG-Pu or w/o U-235

L-0 4.74						
M-56 4.71	M-56 4.71					
L-48 3.91	M-24 6.00	M-56 4.71				
M-56 4.71	L-48 3.91	M-56 4.71	M-56 4.71			
M-56 4.71	M-56 4.71	L-48 3.91	M-56 4.71	L-48 3.91		
M-56 4.71	L-48 3.91	M-56 4.71	L-48 3.91	M-56 4.71	L-48 3.91	
L-48 3.91	M-56 4.71	L-48 3.91	M-56 4.71	M-24 6.00	L-0 4.74	M-56 4.71
M-56 4.71	L-0 4.74	M-24 6.00	L-0 4.74	M-24 6.00	M-56 4.71	
M-56 4.71	M-24 6.00	M-56 4.71	M-24 6.00			

Twice-Burnt WG-MOX
Once-Burnt WG-MOX
Fresh LEU

FIGURE 20. Initial Mixed Core Loading Pattern

Assembly Burnup (GWd/MTM)
Assembly Power
Peak Pin Power

0.00 1.09 1.23						
39.47 0.80 1.00	39.55 0.79 0.83					
0.00 1.08 1.20	18.41 1.18 1.59	41.63 0.88 0.95				
39.90 1.00 1.17	0.00 1.18 1.30	21.58 1.13 1.43	21.43 1.11 1.21			
21.09 1.13 1.25	21.44 1.21 1.46	0.00 1.22 1.33	22.26 1.20 1.43	0.00 1.24 1.35		
19.14 1.29 1.57	0.00 1.26 1.38	37.67 1.06 1.27	0.00 1.16 1.29	22.60 1.17 1.44	0.00 1.22 1.31	
0.00 1.26 1.39	21.82 1.26 1.51	0.00 1.18 1.31	38.57 0.95 1.16	26.66 1.03 1.38	0.00 1.11 1.44	22.31 0.54 1.17
37.52 0.90 1.19	0.00 1.26 1.53	20.38 1.12 1.58	0.00 1.06 1.32	16.41 0.72 1.18	40.72 0.35 0.76	
39.85 0.41 0.66	30.89 0.34 1.07	41.48 0.41 0.68	28.63 0.41 0.96			

FIGURE 21. Initial Mixed Core BOC Conditions

Assembly Burnup (GWd/MTM)
Assembly Power
Peak Pin Burnup (GWd/MTM)

18.93 1.17 20.61						
53.80 0.90 56.55	53.70 0.89 55.25					
19.53 1.17 21.81	38.64 1.21 46.76	57.04 0.93 57.86				
57.13 1.02 59.01	20.77 1.20 23.01	40.83 1.12 47.48	40.23 1.10 42.17			
40.24 1.11 42.32	41.79 1.17 47.53	21.21 1.21 23.21	42.42 1.16 48.38	21.45 1.22 23.49		
40.32 1.20 44.35	21.52 1.22 23.67	55.60 1.05 60.18	20.39 1.19 22.52	42.18 1.14 48.68	20.77 1.20 22.63	
21.12 1.19 23.34	42.26 1.16 48.00	20.19 1.17 22.44	54.54 0.96 58.53	43.93 1.04 56.39	18.20 1.07 23.44	31.66 0.60 42.78
52.20 0.87 59.55	19.87 1.14 23.20	38.60 1.08 51.99	17.38 1.04 20.80	28.70 0.78 41.72	46.97 0.41 53.39	
47.03 0.47 51.84	40.04 0.58 44.52	48.71 0.47 52.46	35.86 0.48 41.78			

FIGURE 22. Initial Mixed Core EOC Conditions

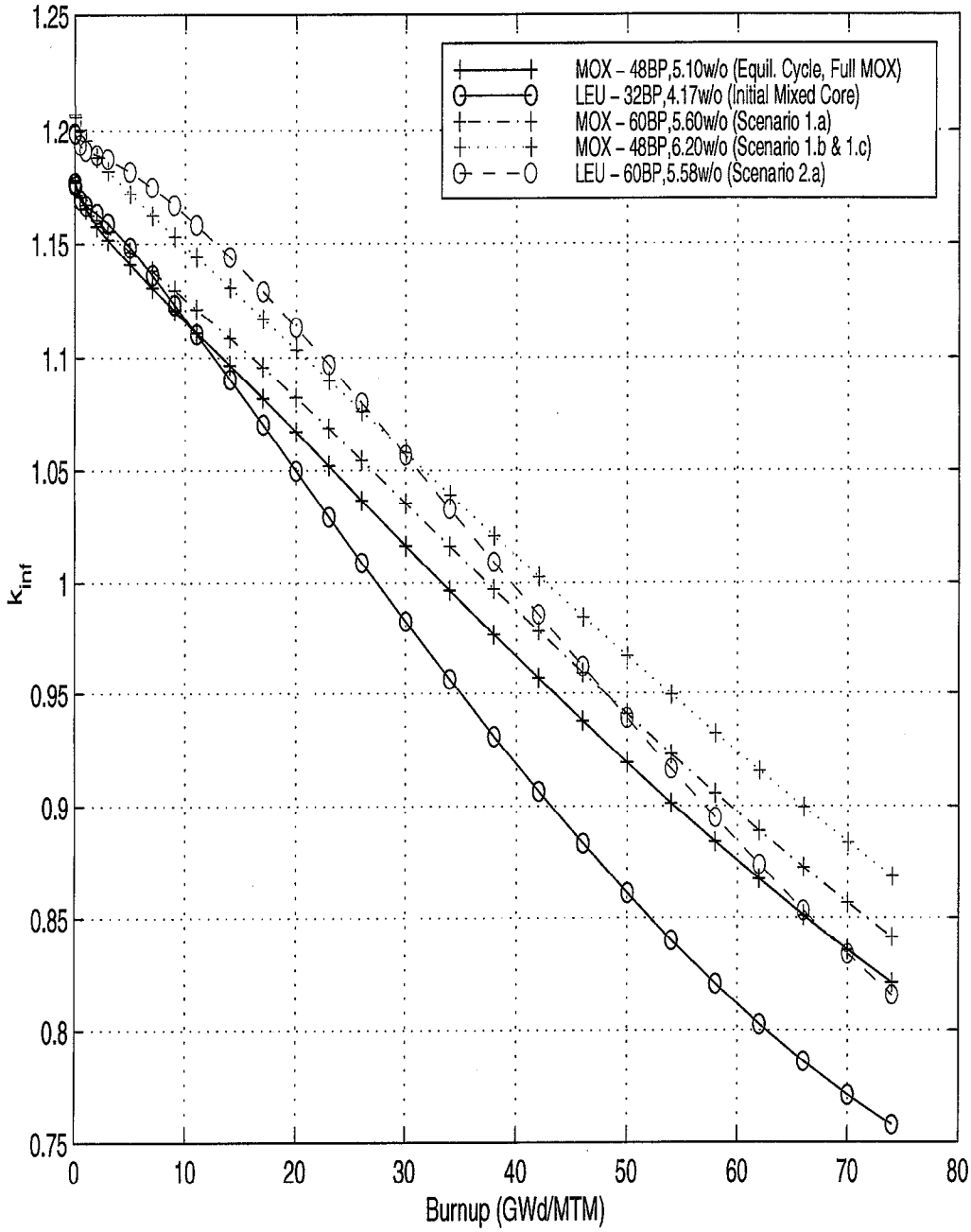

FIGURE 23. k_{inf} versus Burnup for MOX and LEU Assemblies

6. Subsequent Mixed LEU-MOX Cores

Starting with the initial mixed LEU-MOX core defined in Section 5, three different scenarios are introduced in regard to availability of MOX feed assemblies in the subsequent cycle: (1) assume that MOX feed batches are available, (2) assume that MOX feed batches continue to be unavailable, and (3) assume that only one of the two MOX feed batches is available, requiring substitution with an LEU feed batch. For all three scenarios, problems have been encountered in finding LPs which satisfy all constraints. Do note that we are limiting LEU lattice designs to standard ABB-CE designs which employ only two different LEU enrichments for each lattice using an "island" type pin-wise enrichment layout as depicted in Figure 19. This was done to determine if acceptable LPs could be determined without the need to develop new and more complex lattice designs. We have also retained the original MOX lattice designs developed by ABB-CE for the equilibrium cycle, full MOX core.

6.1 Scenario 1: MOX Feed Batches Available for Subsequent Cycle

For this scenario, we desire to approximately preserve the differences in the number of BP rods and average enrichment between the dominant and non-dominant MOX feed batches as in the equilibrium cycle, full MOX core. By preserving these differences, we hope that we can smoothly transition back to the equilibrium cycle, full MOX core as quickly as possible. The assumption is that the lattice k_∞ is linearly dependent upon either average feed enrichment or at BOC number of BP rods (Figure 24). Therefore, by maintaining the enrichment and BP differences we maintain the difference in k_∞ between the dominant and non dominant feed batches at BOC and EOC. The optimum LP found using FORMOSA-P, denoted as Scenario 1.a, feed fuel loading and core characteristics are summarized in Figure 25 and Table 17. This LP has a very high peak pin power in the feed MOX assemblies adjacent to once-burnt LEU assemblies

(Figure 26 and Figure 27). It also exhibits moderate peak pin burnup violations (Figure 28). There is a trade off between satisfying the peak pin power limit and the peak pin discharge burnup limit. The LP for Scenario 1.a emphasizes minimization of the dominant batch feed enrichment, the FORMOSA-P objective function selected, required to satisfy the cycle energy requirement. This is accomplished by loading the most highly burnt assemblies on the core periphery, which also minimizes peak pin discharge burnups. This results in once burnt LEU assemblies adjacent to feed MOX assemblies in the core interior, resulting in high power peaking attributed to interfacial effects of having a feed MOX assembly adjacent to a once burnt LEU assembly. This is clearly illustrated in Figure 27. Indeed the pin-wise power gradient is so severe, it casts doubt on the ability of the quartic flux expansion used in FORMOSA-P to correctly treat nodal diffusion coupling.

Further FORMOSA-P optimization have been performed with the objective of minimizing the peak pin power, not imposing either the peak pin discharge burnup or maximum soluble boron constraints. The enrichment for the dominant feed batch is allowed to vary in order to satisfy the cycle energy requirement. The number of BP rods is also allowed to vary in both feed batches. This is a very unconstrained problem, hence should render the lowest peak pin power achievable.

Two different split feed enrichments have been considered. In one case, denoted as Scenario 1.b, the non-dominant batch average feed enrichment is set to 6.15 w/o. Figure 30 through Figure 32 and Table 17 summarize the attributes of the optimum LP determined for this case. It turns out that for the optimum LP determined, the dominant batch average feed enrichment required to satisfy the cycle energy requirement is also 6.15 w/o, so a non-split feed enrichment results. The lowest peak pin power found for this case is 1.82, which is an improvement over Scenario 1.a which exhibited a peak pin power of 1.96; however, this value is still considerable above the maximum acceptable value of 1.64 reported by ABB C-E. Do note that now high pin powers are also observed in feed

assemblies that are totally surrounded by twice burnt MOX assemblies. The associated peak pin discharge burnup of ~64 GWd/T, above the 60 GWd/T limit, is comparable to the Scenario 1.a value. Again, severe pin-wise power gradients are observed for MOX assemblies adjacent to LEU assemblies, casting doubt on both the NEM and pin-power reconstruction methodologies.

The other case, denoted Scenario 1.c, the non-dominant batch average feed enrichment is set at 6.45 w/o. The thought was that since the more reactive non-dominant batch has fewer assemblies, they all could be placed close to the core periphery or surrounded by very high burnup assemblies to reduce their pin power peaks. The less reactive dominant batch would now have a better chance of occupying interior core locations surrounded by less burnt assemblies and still display acceptable power peaking. Figure 33 through Figure 35 and Table 17 summarize the attributes of the optimum LP determined for this case. The dominant feed batch average enrichment required to satisfy the cycle energy requirement for the optimum LP was determined to be 6.15 w/o. However, the peak pin power only declined modestly to 1.73, still considerable above the limit of 1.64, with the associated peak pin discharge burnup increasing to ~66 GWd/T. Again note that now high pin powers are also observed in feed assemblies that are totally surrounded by twice burnt MOX assemblies.

The assembly averaged feed region enrichments for Scenarios 1.a, 1.b and 1.c are 5.60, 6.15 and 6.24 w/o WGPu, respectively. From these values, it appears that Scenarios 1.b and 1.c require much more reactivity to be installed in the feed region then Scenario 1.a. This is not the case, since the number of Erbia pin varies among these cases. Recall that Erbia pins utilize LEU as the fuel, hence, the number of Erbia pins determines the fraction of the feed region composed of LEU and MOX fuel. This in turn impacts the feed region reactivity as a function of burnup. Figure 23 displays the feed region (assembly averaged) reactivity versus burnup for Scenarios 1.a and 1.c. Examining the reactivity at the feed region average burnup at EOC, which is about 20 GWd/MTM, we note that

Scenario 1.a and 1.c feed region reactivities differ by less than 2.0% $\Delta\rho$, with Scenario 1.c having the higher reactivity consistent with its associated higher leakage LP. This confirms that the feed enrichments predicted by FORMOSA-P are consistent among the different cases associated with Scenario 1.

All these results are based upon the MOX lattice designs developed by ABB C-E for the equilibrium cycle, full MOX core and standard ABB-CE LEU lattice designs. Up to 88 Erbia pins per MOX assembly were allowed during the optimization in an attempt to hold down assembly power peaking. Needless to say, this proved unsuccessful. We therefore conclude that either or both the MOX and LEU within lattice pin enrichment distributions may need to be modified to minimize the strong MOX-LEU interfacial effect. The option to insert fresh or partially depleted discrete burnable poison pins in the burnt assemblies adjacent to fresh MOX assemblies with high pin powers does not exist for ABB C-E lattices, since discrete burnable poison pins displace fuel rods in their design, hence cannot be easily added after fuel fabrication.

So far the number of feed assemblies has been held fixed at the minimum number required as dictated by the region average discharge burnup limit. If more feed assemblies were employed, the average feed enrichment could be lowered, which would reduce power peaking in these assemblies. But this is a very expensive approach to solving this problem. The usage of more feed assemblies would also allow discharge of the highest burnt assemblies; thereby, perhaps avoiding peak pin discharge burnup limit violations.

Another alternative is to increase the average feed enrichment for the initial mixed LEU-MOX core above that required to just satisfy the cycle energy requirement, which will modestly increase fuel cycle cost. This will result in increased reactivity carry-forward in the once burnt LEU assemblies in the subsequent cycle, thereby decreasing the average feed enrichment required, which in turn will reduce power peaking in the feed assemblies.

Finally, note that most feed reactivities for Scenarios 1.a, 1.b and 1.c LPs are much higher than for the equilibrium cycle, full MOX core, implying that criticality limits during fuel fabrication and on-site storage may be violated. This can be observed in Figure 23 which presents the feed region average reactivity as a function of burnup, noting that some individual assemblies will have higher reactivities than the region average reactivity. There already exists interest among fuel vendors in increasing the ^{235}U enrichment limit at their fuel fabrication facilities, so action on this interest may address the maximum enrichment violation. The spent fuel pool ^{235}U enrichment limit is viewed a less challenging limit to relax. The same interest may extend to WGPu, where the fuel material conversion and fabrication plants have not yet been designed. In any case, utilizing of more feed assemblies or increasing the average feed enrichment of the initial mix LEU-MOX core would also address the criticality concern by reducing the feed enrichments required in the subsequent cycle. Why the feed region reactivity is so high is because of the lower reactivity carry-forward of the once burnt LEU assemblies. This occurs not only because the assembly reactivity decreases faster with burnup for LEU versus MOX assemblies, but also because as noted earlier the average feed enrichment of the once burnt LEU assemblies is lower than for an equilibrium cycle, full LEU core.

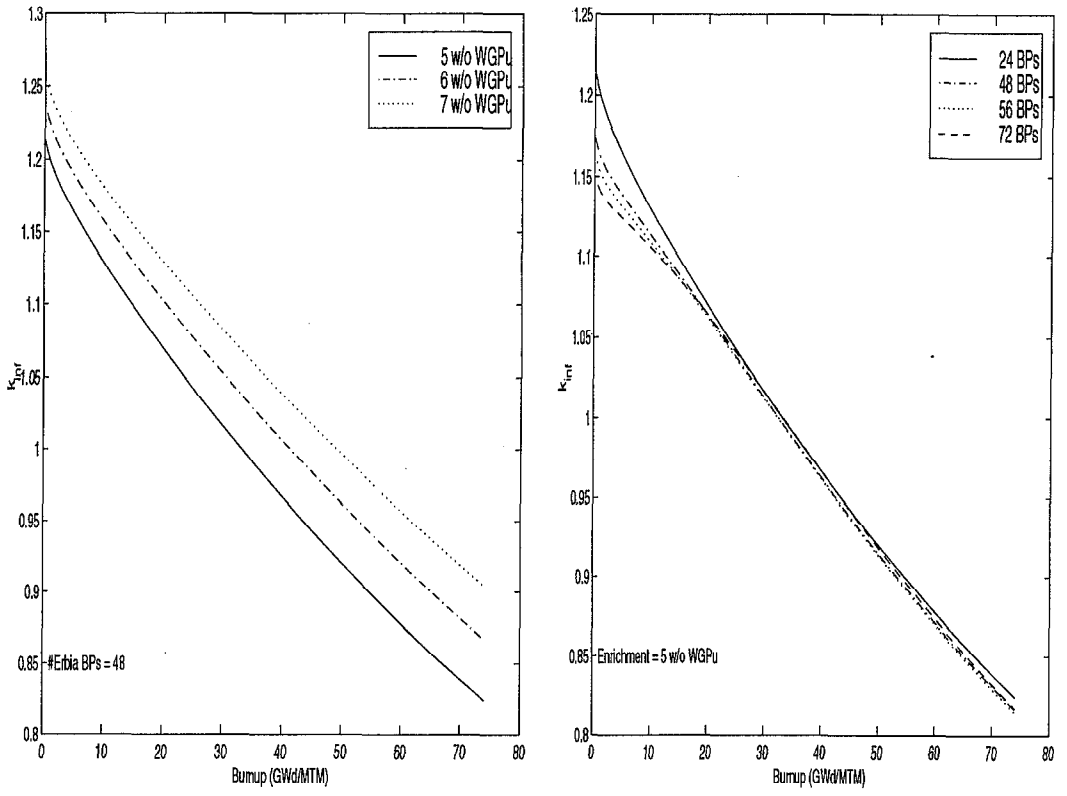

FIGURE 24. MOX assembly reactivity versus burnup for different WGPu average assembly enrichments and BP loadings

TABLE 17: Various Scenarios' Mixed LEU-MOX Cores Performance Characteristics

	Scenario					
Characteristic	**1.a**	**1.b**	**1.c**	**2.a**	**2.b**	**3**
Maximum $F_{\Delta H}$	**1.96**	**1.82**	**1.73**	1.60	**1.64**	**1.64**
Boron Worth(pcm/PPM)						
HFP, BOC	-5.14	-2.07	-3.961	-5.56	-5.43	-5.09
HFP, EOC	-5.79	-5.88	-5.56	-7.40	-7.41	-6.75
MTC (pcm/^{o}F)						
HFP, BOC	-21.06	-20.04	-21.68	-14.15	-12.68	-16.42
HFP, EOC	-41.07	-41.20	-42.26	-39.96	-39.77	-40.05
Maximum Soluble Boron (ppm)	1987	1994	1975	1798	1926	1801
Maximum Pin Discharge Burnup (MWd/MTHM)	**63,696**	**64,273**	**66,378**	**64,650**	**62,893**	**65,119**

MOX or LEU - # Erbia BPs
w/o WG-Pu or w/o U-235

M-24 6.25						
M-56 4.71	L-48 3.91					
M-24 5.30	L-48 3.91	M-56 4.71				
L-48 3.91	M-24 5.30	M-24 6.00	M-56 4.71			
M-56 4.71	L-48 3.91	M-88 6.25	L-48 3.91	M-72 5.30		
L-48 3.91	M-72 5.30	M-56 4.71	M-88 5.30	M-24 6.00	M-56 5.30	
M-72 5.30	L-0 4.74	M-88 5.30	M-88 6.25	M-56 6.25	L-0 4.74	M-56 4.71
L-48 3.91	M-24 5.30	L-48 3.91	L-0 4.74	L-48 3.91	M-56 4.71	
M-56 4.71	M-24 6.00	M-56 4.71	M-56 4.71			

Twice-Burnt WG-MOX
Once-Burnt LEU
Fresh WG-MOX

FIGURE 25. Scenario 1.a Loading Pattern

0.00 1.08 1.24						
40.23 **0.76** **0.88**	19.52 0.78 0.86					
0.00 1.29 **1.72**	21.48 0.85 1.00	**40.29** **0.78** **0.92**				
21.40 0.99 1.06	0.00 1.39 **1.73**	**38.64** **0.98** **1.13**	**40.23** **0.89** **1.12**			
31.70 **1.03** **1.23**	20.37 1.03 1.13	0.00 1.45 **1.95**	20.73 1.07 1.21	0.00 1.55 **1.90**		
21.08 1.06 1.16	0.00 1.45 **1.96**	**41.77** **1.05** **1.15**	0.00 1.56 **1.94**	**28.74** **1.40** **1.53**	0.00 1.43 **1.71**	
0.00 1.48 **1.96**	19.86 1.24 1.36	0.00 1.43 **1.85**	0.00 1.53 **1.88**	0.00 1.42 **1.79**	17.40 0.85 1.20	**40.83** **0.35** **0.76**
20.74 0.83 1.03	0.00 1.18 **1.75**	21.17 0.76 0.98	18.21 0.79 1.05	20.17 0.53 0.87	**42.24** **0.29** **0.66**	
40.83 **0.36** **0.68**	**38.61** **0.41** **0.72**	**42.17** **0.30** **0.61**	**42.40** **0.21** **0.46**			

Assembly Burnup (GWd/MTM)
Assembly Power
Peak Pin Power

bold denotes violation

FIGURE 26. Scenario 1.a Core BOC Conditions

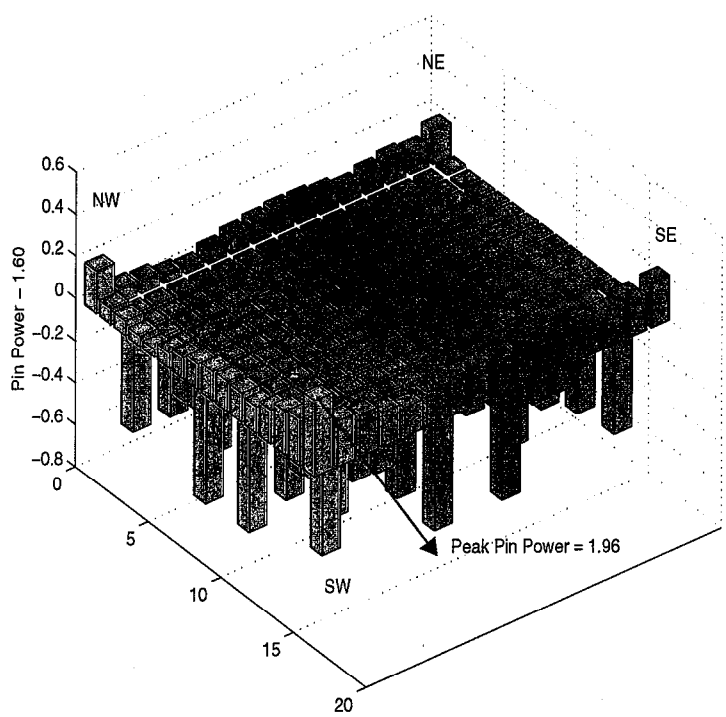

FIGURE 27. Scenario 1.a Pin-Wise Power Distribution

(Assembly location is shown by **bold** box in Figure 26)

18.25 1.15 21.50						
53.45 0.84 56.27	32.80 0.82 35.18					
20.45 1.21 28.72	35.50 0.83 39.53	53.76 0.84 58.80				
37.04 0.89 40.60	21.97 1.27 29.66	55.41 1.01 63.70	55.78 0.94 62.30			
48.86 1.01 57.39	37.16 0.95 41.25	24.96 1.47 32.82	38.48 0.99 42.98	26.03 1.48 31.52		
38.21 0.95 41.60	24.51 1.42 31.87	60.13 1.09 63.19	26.85 1.55 30.72	51.89 1.32 63.14	23.91 1.37 27.11	
24.44 1.40 31.91	39.57 1.09 44.59	24.84 1.46 29.87	26.58 1.56 29.11	24.15 1.41 29.43	32.01 0.87 39.44	47.48 0.44 58.82
34.61 0.81 38.81	19.39 1.14 29.68	34.49 0.80 39.16	32.29 0.86 39.10	29.89 0.61 35.26	47.79 0.37 59.33	
47.52 0.44 53.65	46.07 0.49 55.30	47.59 0.39 54.05	46.76 0.31 57.14			

Assembly Burnup (GWd/MTM)
Assembly Power
Peak Pin Burnup (GWd/MTM)

bold denotes violation

FIGURE 28. Scenario 1.a Core EOC Conditions

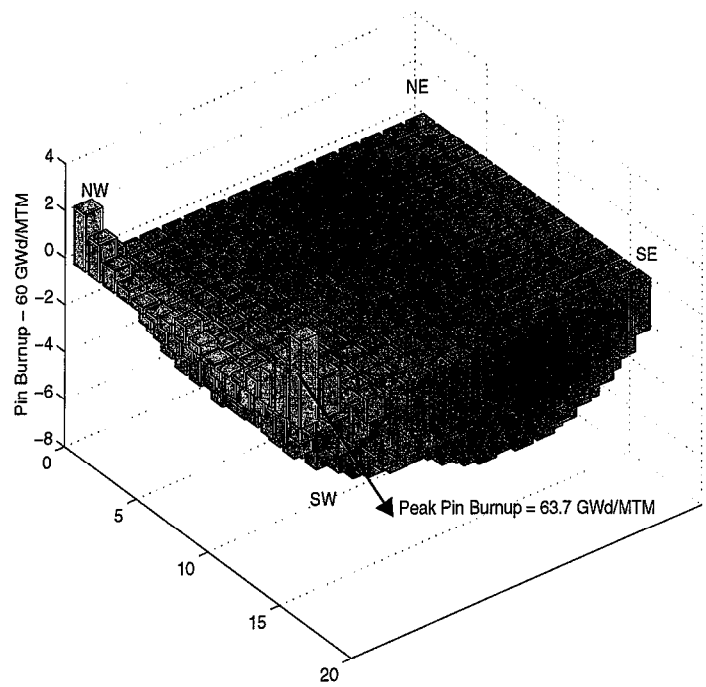

FIGURE 29. Scenario 1.a Pin-Wise Discharge Burnup Distribution

(Assembly location is shown by **bold** box in Figure 28)

MOX or LEU - # Erbia BPs
w/o WG-Pu or w/o U-235

M-56 6.15						
L-48 3.91	L-48 3.91					
M-56 6.15	L-0 4.74	M-56 4.71				
M-56 4.71	M-88 6.15	L-48 3.91	M-56 4.71			
L-48 3.91	M-24 6.00	M-56 6.15	L-48 3.91	M-56 6.15		
M-56 4.71	M-56 6.15	M-56 4.71	L-0 4.74	M-56 4.71	M-48 6.15	
M-56 6.15	M-24 6.00	M-72 6.15	L-0 4.74	M-56 6.15	M-0 6.15	M-56 4.71
M-56 4.71	M-0 6.15	L-48 3.91	M-0 6.15	L-48 3.91	M-56 4.71	
L-48 3.91	L-48 3.91	M-24 6.00	M-56 4.71			

Twice-Burnt WG-MOX
Once-Burnt LEU
Fresh WG-MOX

FIGURE 30. Scenario 1.b Core Loading Pattern

0.00 1.26 **1.65**						
20.74 0.91 0.99	21.08 0.92 1.00					
0.00 1.41 **1.76**	18.21 1.10 1.27	40.83 0.85 0.98				
40.29 0.97 1.08	0.00 1.40 **1.80**	21.48 0.89 1.04	40.23 0.85 0.99			
21.40 0.98 1.03	28.74 1.23 1.38	0.00 1.41 **1.74**	21.17 0.94 1.04	0.00 1.34 **1.69**		
40.83 1.03 1.11	0.00 1.48 **1.68**	42.24 0.99 1.09	17.40 1.17 1.25	42.40 0.97 1.07	0.00 1.44 1.64	
0.00 1.47 **1.68**	38.64 1.17 1.29	0.00 1.45 **1.82**	19.86 1.15 1.30	0.00 1.32 **1.74**	0.00 1.18 1.60	40.23 0.45 0.84
31.70 0.88 1.04	0.00 1.24 **1.68**	20.37 0.82 1.02	0.00 1.09 1.77	20.17 0.56 0.84	41.77 0.33 0.69	
19.52 0.42 0.64	20.73 0.41 0.63	38.61 0.42 0.85	42.17 0.27 0.53			

Assembly Burnup (GWd/MTM)
Assembly Power
Peak Pin Power

bold denotes violation

FIGURE 31. Scenario 1.b Core BOC Conditions

22.18 1.28 30.68						
36.45 0.88 38.68	36.85 0.88 38.73					
24.35 1.40 32.04	36.73 1.04 42.20	56.14 0.91 62.26				
57.58 1.02 **61.24**	24.71 1.44 31.46	36.97 0.89 41.66	55.30 0.91 60.40			
38.00 0.94 41.12	49.68 1.22 63.06	24.17 1.41 30.98	36.94 0.90 40.12	22.82 1.35 30.40		
58.52 1.05 62.20	24.95 1.45 27.67	59.33 1.01 63.65	36.34 1.07 39.94	58.72 0.98 63.94	23.27 1.36 26.90	
24.54 1.44 27.70	58.24 1.16 64.27	24.15 1.41 30.82	38.17 1.04 42.44	21.86 1.30 29.42	18.84 1.12 23.53	47.94 0.49 54.29
46.96 0.93 52.73	20.59 1.23 28.26	34.25 0.82 39.05	17.95 1.08 30.59	29.85 0.61 35.39	47.77 0.40 57.85	
27.41 0.53 30.89	28.44 0.51 32.96	46.33 0.51 55.27	47.18 0.34 52.58			

Assembly Burnup (GWd/MTM)
Assembly Power
Peak Pin Burnup (GWd/MTM)

bold denotes violation

FIGURE 32. Scenario 1.b Core EOC Conditions

MOX or LEU - # Erbia BPs
w/o WG-Pu or w/o U-235

M-24 6.45						
L-48 3.91	l-48 3.91					
M-48 6.15	L-48 3.91	M-56 4.71				
M-56 4.71	M-48 6.15	L-0 4.74	M-56 4.71			
L-48 3.91	M-24 6.00	L-0 4.74	M-56 4.71	M-48 6.15		
M-56 4.71	M-48 6.15	M-24 6.00	M-48 6.45	M-56 4.71	M-56 6.15	
M-48 6.15	M-56 4.71	M-56 6.15	M-24 6.00	M-56 6.15	M-56 6.45	M-56 4.71
L-48 3.91	M-24 6.15	L-48 3.91	M-24 6.45	L-48 3.91	L-48 3.91	
M-56 4.71	L-0 4.74	M-56 4.71	L-48 3.91			

Twice-Burnt WG-MOX
Once-Burnt LEU
Fresh WG-MOX

FIGURE 33. Scenario 1.c Core Loading Pattern

Assembly Burnup (GWd/MTM)
Assembly Power
Peak Pin Power

bold denotes violation

0.00 1.31 **1.69**						
21.08 0.87 0.93	20.74 0.85 0.92					
0.00 1.32 **1.63**	20.37 0.90 1.02	31.70 0.92 1.07				
40.23 0.94 1.07	0.00 1.38 **1.70**	18.21 1.06 1.21	40.83 0.82 0.92			
21.40 0.93 0.99	38.64 1.12 1.40	19.86 1.14 1.25	42.40 0.91 1.08	0.00 1.39 **1.63**		
40.83 0.99 1.07	0.00 1.49 **1.72**	28.74 1.32 1.61	0.00 1.53 **1.73**	42.17 1.01 1.11	0.00 1.42 **1.67**	
0.00 1.44 **1.69**	42.24 0.99 1.09	0.00 1.49 **1.73**	38.61 1.14 1.35	0.00 1.33 **1.65**	0.00 1.12 1.54	40.29 0.42 0.78
19.52 0.86 1.03	0.00 1.25 **1.70**	20.17 0.83 1.01	0.00 1.10 **1.66**	21.48 0.56 0.84	20.73 0.35 0.69	
40.23 0.42 0.73	17.40 0.50 0.78	41.77 0.36 0.66	21.17 0.28 0.52			

FIGURE 34. Scenario 1.c Core BOC Conditions

Assembly Burnup (GWd/MTM)
Assembly Power
Peak Pin Burnup (GWd/MTM)

bold denotes violation

21.76 1.24 30.56						
35.89 0.84 38.76	35.38 0.83 36.94					
22.41 1.30 30.02	35.62 0.86 39.38	47.65 0.93 53.65				
56.40 0.95 58.55	23.00 1.32 30.39	35.69 0.98 41.63	55.24 0.86 63.26			
36.92 0.88 39.94	57.30 1.08 65.90	38.24 1.02 43.01	58.14 0.94 63.83	23.55 1.39 28.65		
57.63 0.99 62.05	24.34 1.39 27.78	50.27 1.23 60.56	25.24 1.45 28.53	59.71 1.05 62.78	24.30 1.45 28.77	
23.76 1.38 29.15	59.06 1.00 62.46	24.67 1.42 29.37	57.77 1.13 66.38	22.79 1.36 27.27	19.80 1.22 24.97	48.19 0.53 55.39
34.02 0.85 38.60	20.57 1.22 29.05	34.16 0.82 38.93	18.52 1.12 28.23	31.55 0.64 37.23	27.45 0.45 32.40	
48.04 0.51 55.59	26.42 0.59 30.59	48.66 0.46 58.71	26.61 0.37 30.89			

FIGURE 35. Scenario 1.c EOC Conditions

6.2 Scenario 2: MOX Feed Batches Continue to be Unavailable for Subsequent Cycle

For this scenario, LEU feed batches substitute for MOX feed batches. We preserve the differences in the average enrichment between the dominant and non-dominant LEU feed batches as in the initial mixed core. The number of BP rods is allowed to vary for both non-dominant and dominant batches, providing FORMOSA-P with an enlarged decision space. No LP has been found that satisfies all constraints, with results presented for two of the better LPs determined by FORMOSA-P, denoted Scenario 2.a and 2.b, in Table 17 and Figure 36 through Figure 42. First note that the ^{235}U feed region enrichments required to satisfy the cycle energy requirement are above 5.0 w/o, which is the current limit in regard to both fuel fabrication and spent fuel storage as limited by criticality constraints. The reasons for this behavior are the same as explained in Section 6.1. Indeed, note in Figure 23 that the feed region averaged reactivity at the EOC region average burnup (~20 GWd/MTM) are nearly the same for Scenario 1.c and 2.a, indicating consistency in results.

Again note that there is a trade off between satisfying the peak pin power limit and the peak pin discharge burnup limit. Scenario 2.a LP (Figure 37 and Figure 38) shows that the peak pin power constraint is satisfied, but that moderate peak pin discharge burnup violations exist. The peak pin burnup violations occur in pins adjacent to feed LEU assemblies (Figure 39). This figure indicates that pin-wise burnups within assemblies with violations display very strong burnup gradients due to LEU-MOX interfacial effects as observed earlier. Scenario 2.b LP (Figure 41 and Figure 42) is close to satisfying the peak pin discharge burnup limit. Using 1.64 as the limit, the peak pin power in LP in Scenario 2.b is within the pin power limit imposed. Do note that ABB-CE in developing equilibrium cycle, full MOX core designs judged radial peaking factors as high as 1.64 as acceptable. The approaches noted earlier for Scenario 1 should prove effective in removing these moderate peak pin violations and perhaps avoiding criticality limit violations.

MOX or LEU - # Erbia BPs
w/o WG-Pu or w/o U-235

L-72 6.10						
L-48 3.91	M-56 4.71					
L-72 5.35	L-0 4.74	M-56 4.71				
L-48 3.91	L-72 5.35	M-24 6.00	L-48 3.91			
M-56 4.71	L-48 3.91	L-72 5.35	M-56 4.71	L-72 5.35		
M-56 4.71	L-72 5.35	L-48 3.91	L-72 5.35	L-48 3.91	L-72 5.35	
L-72 5.35	L-48 3.91	L-72 5.35	L-0 4.74	L-0 4.74	L-24 6.10	M-56 4.71
L-48 3.91	L-24 6.10	L-48 3.91	L-24 6.10	M-24 6.00	M-56 4.71	
M-56 4.71	M-24 6.00	M-56 4.71	M-56 4.71			

Twice-Burnt WG-MOX
Once-Burnt LEU
Fresh WG-MOX

FIGURE 36. Scenario 2.a Loading Pattern

0.00 1.26 1.34						
21.40 0.91 1.01	40.29 0.91 1.03					
0.00 1.40 1.57	17.40 1.20 1.38	31.70 1.02 1.18				
19.52 1.08 1.20	0.00 1.41 1.57	28.74 1.19 1.48	21.08 0.93 0.98			
40.23 0.90 1.07	21.48 1.02 1.13	0.00 1.38 1.54	40.83 0.98 1.16	0.00 1.33 1.54		
40.23 0.94 1.09	0.00 1.35 1.54	20.17 1.12 1.20	0.00 1.41 1.57	20.73 1.08 1.15	0.00 1.39 1.54	
0.00 1.30 1.43	21.17 1.05 1.13	0.00 1.39 1.57	19.86 1.19 1.30	18.21 1.07 1.21	0.00 1.18 **1.60**	41.77 0.43 0.89
20.74 0.83 1.02	0.00 1.24 1.55	20.37 0.82 1.03	0.00 1.09 1.53	38.64 0.59 1.08	42.40 0.32 0.70	
41.77 0.36 0.64	38.61 0.43 0.84	42.24 0.33 0.62	42.17 0.26 0.55			

Assembly Burnup (GWd/MTM)
Assembly Power
Peak Pin Power

FIGURE 37. Scenario 2.a Core BOC Conditions

21.93 1.34 23.34						
36.44 0.88 39.00	55.51 0.92 61.80					
23.75 1.37 25.81	36.40 1.07 39.56	48.61 1.00 60.39				
36.95 0.98 39.41	24.03 1.38 25.91	48.68 1.17 63.02	36.55 0.90 40.12			
55.84 0.94 61.65	38.31 0.95 40.88	23.99 1.39 26.38	57.76 1.01 64.65	23.32 1.37 26.00		
56.73 1.00 61.24	23.75 1.39 26.39	38.50 1.02 40.98	24.26 1.40 26.22	38.18 0.98 40.77	23.77 1.38 25.95	
23.25 1.38 24.95	38.49 0.98 40.96	24.13 1.40 26.39	38.74 1.07 42.07	35.37 0.99 41.76	19.81 1.19 25.71	49.49 0.51 60.15
34.96 0.85 38.08	21.24 1.28 26.18	34.30 0.84 38.00	18.50 1.13 25.26	48.88 0.65 60.90	48.12 0.38 55.97	
48.57 0.46 57.02	46.54 0.53 55.47	48.40 0.42 58.50	47.08 0.34 58.14			

Assembly Burnup (GWd/MTM)
Assembly Power
Peak Pin Burnup (GWd/MTM)

bold denotes violation

FIGURE 38. Scenario 2.a Core EOC Conditions

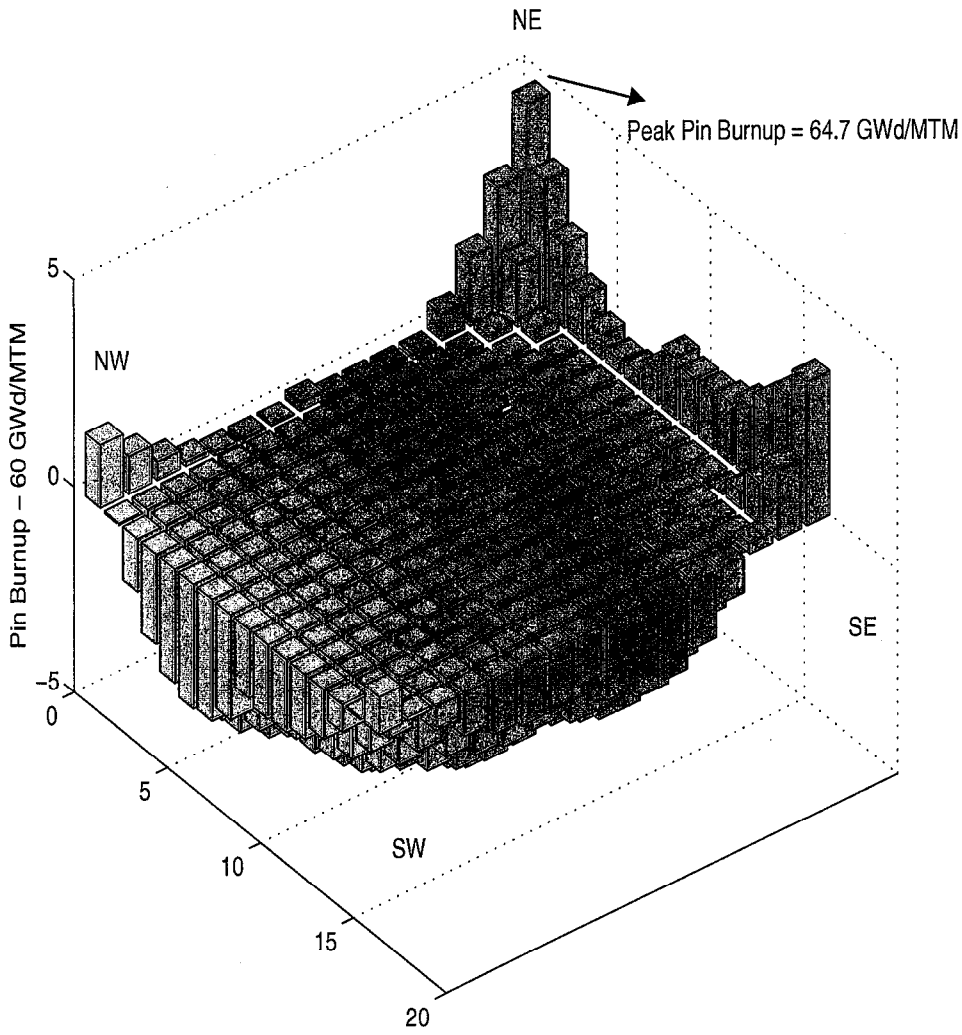

FIGURE 39. Scenario 2.a: Pin-Wise Discharge Burnup Distribution

(Assembly location is shown by **bold** box in Figure 38)

MOX or LEU - # Erbia BPs
w/o WG-Pu or w/o U-235

L-24 6.10						
M-56 3.91	L-48 3.91					
L-48 5.35	L-0 4.74	L-48 3.91				
L-48 3.91	L-32 5.35	M-24 6.00	M-56 3.91			
M-56 4.71	L-48 3.91	L-60 5.35	L-48 3.91	L-32 5.35		
M-56 4.71	L-72 5.35	L-0 4.74	L-72 5.35	L-48 3.91	L-32 5.35	
L-48 5.35	L-48 3.91	L-72 5.35	L-0 4.74	L-48 3.91	L-24 6.10	M-56 4.71
L-48 3.91	L-32 6.10	M-24 6.00	L-24 6.10	M-24 6.00	M-56 4.71	
M-56 4.71	M-24 6.00	M-56 4.71	M-56 4.71			

Twice-Burnt WG-MOX
Once-Burnt LEU
Fresh WG-MOX

FIGURE 40. Scenario 2.b Loading Pattern

0.00 1.40 1.56						
31.70 **1.02** **1.23**	21.08 0.95 1.03					
0.00 1.43 1.57	18.21 1.18 1.36	20.74 0.88 0.99				
21.40 1.04 1.17	0.00 1.41 1.59	**41.77** **0.86** **1.09**	**40.23** **0.82** **1.05**			
40.29 **0.88** **1.05**	20.37 1.02 1.16	0.00 1.37 1.58	20.17 1.04 1.19	0.00 1.50 **1.64**		
40.23 **0.95** **1.14**	0.00 1.37 1.59	19.86 1.33 1.44	0.00 1.45 **1.62**	21.48 1.07 1.18	0.00 1.43 1.59	
0.00 1.39 1.49	21.17 1.09 1.20	0.00 1.44 **1.62**	17.40 1.22 1.37	20.73 0.86 1.07	0.00 1.09 1.52	**40.82** **0.40** **0.85**
19.52 0.87 1.09	0.00 1.26 1.57	**28.74** **0.99** **1.54**	0.00 1.07 1.51	**38.64** **0.54** **1.02**	**42.24** **0.28** **0.59**	
40.83 **0.38** **0.69**	**38.61** **0.45** **0.86**	**42.17** **0.34** **0.56**	**42.40** **0.26** **0.56**			

Assembly Burnup (GWd/MTM)
Assembly Power
Peak Pin Power

bold denotes violation

FIGURE 41. Scenario 2.b Core BOC Conditions

22.57 1.35 23.90						
48.38 **1.01** **56.02**	36.20 0.89 38.89					
23.42 1.36 25.06	36.70 1.06 40.77	35.18 0.86 37.50				
38.03 0.95 40.63	23.21 1.34 25.04	**56.57** **0.91** **62.89**	**54.57** **0.88** **60.96**			
55.62 **0.94** **61.89**	37.20 0.96 39.91	23.69 1.37 26.17	37.21 0.96 40.21	24.58 1.38 26.05		
57.02 **1.01** **61.99**	24.24 1.40 26.96	41.05 1.16 43.97	24.90 1.41 26.58	38.60 0.96 41.21	23.53 1.36 25.87	
24.23 1.40 25.87	39.23 1.01 41.71	25.03 1.43 27.02	37.07 1.11 41.21	35.15 0.86 37.88	18.76 1.16 25.01	**48.24** **0.50** **59.66**
34.63 0.89 37.67	21.95 1.31 27.31	**46.07** **1.05** **55.38**	18.67 1.15 25.14	**48.37** **0.64** **60.06**	**47.51** **0.37** **56.85**	
48.05 **0.49** **54.69**	**47.00** **0.56** **55.71**	**48.68** **0.45** **58.05**	**47.50** **0.36** **58.10**			

Assembly Burnup (GWd/MTM)
Assembly Power
Peak Pin Burnup (GWd/MTM)

bold denotes violation

FIGURE 42. Scenario 2.b Core EOC Conditions

6.3 Scenario 3: Only One MOX Feed Batch is Available (Dominant Batch) for Subsequent Cycle

For this scenario, the non-dominant MOX feed batch enrichment is retained at 6.0 w/o WGPu as in the equilibrium cycle, full MOX core with 24 BPs. A FORMOSA-P optimization run is then performed to find the enrichment and BP loading for the dominant LEU feed batch which satisfies the cycle energy requirement and all other constraints. Figure 43, Figure 44, and Table 17 summarize the loadings and key core attributes for the best LP determined by FORMOSA-P. Again, no LP has been found which meets all requirements. Similar to other scenarios, the ^{235}U feed enrichment required to satisfy the cycle energy requirement is above 5.0 w/o, the current limit imposed by criticality concerns, requiring action as noted earlier for Scenario 1 to address this concern. The best LP found still has moderate peak pin power and peak pin discharge burnup violations. Again, the approaches noted earlier for Scenario 1 should prove effective in removing these moderate violations.

0.00 1.22 1.39						
38.22 0.93 1.04	20.33 0.97 1.08					
0.00 1.44 1.60	18.08 1.21 1.29	27.99 1.06 1.29				
41.05 1.01 1.13	0.00 1.45 1.63	19.89 1.00 1.13	21.13 0.90 0.99			
20.73 0.99 1.08	20.24 1.09 1.17	0.00 1.42 1.63	42.17 0.95 1.13	0.00 1.40 1.61		
38.98 1.08 1.22	0.00 1.49 1.63	40.55 1.09 1.26	0.00 1.46 1.64	20.56 1.07 1.13	0.00 1.34 1.61	
0.00 1.48 1.57	35.76 1.24 1.53	0.00 1.47 1.64	17.86 1.20 1.34	20.04 1.00 1.27	0.00 0.97 1.63	40.48 0.37 0.71
20.87 0.83 1.05	0.00 1.15 1.63	37.06 0.89 1.32	0.00 0.97 1.58	20.53 0.48 0.81	42.39 0.27 0.58	
40.74 0.37 0.68	20.77 0.38 0.59	41.28 0.38 0.67	41.89 0.24 0.46			

Assembly Burnup (GWd/MTM)
Assembly Power
Peak Pin Power

FIGURE 43. Scenario 3 Core BOC Conditions

19.95 1.20 23151						
53.55 0.92 63518	35.78 0.88 38347					
24.07 1.38 25855	37.05 1.06 42233	45.35 1.00 53446				
58.05 0.99 63625	24.65 1.40 27322	36.32 0.92 39286	36.22 0.87 38508			
36.97 0.91 39072	37.97 0.98 41119	24.76 1.43 27413	58.80 0.99 64594	24.42 1.43 27606		
57.31 1.07 60916	25.68 1.46 27405	59.19 1.09 65119	25.28 1.46 26983	38.05 0.99 41553	23.11 1.37 27416	
25.38 1.46 26878	56.59 1.22 64366	25.11 1.45 27029	37.09 1.09 42132	36.29 0.96 40140	16.76 1.05 28700	47.24 0.46 52243
35.06 0.85 38695	19.77 1.21 28243	52.32 0.94 61833	16.59 1.03 26340	29.08 0.56 33631	47.42 0.35 54076	
47.70 0.48 54604	27.90 0.48 32022	48.29 0.48 57232	46.50 0.32 54367			

Assembly Burnup (GWd/MTM)
Assembly Power
Peak Pin Burnup (GWd/MTM)

FIGURE 44. Scenario 3 Core EOC Conditions

7. Conclusions

HELIOS/FORMOSA-P have been shown to produce consistent predictions of core attributes with those predicted by the ABB-CE DIT/ROCS codes. For the initial mixed LEU-MOX core, starting with the ABB-CE CASE 2 equilibrium cycle, full MOX core, an acceptable LP was determined in regard to satisfying all constraints with the exception of a minor violation of the maximum pin discharge burnup limit (0.2 GWd/MTHM over the limit of 60 GWd/MTHM. For the subsequent cycle, the following three disruption scenarios were examined: (2) complete availability of MOX feed assemblies, (2) complete unavailability of MOX feed assemblies, and (3) partial unavailability (dominant feed batch) of MOX fuel assemblies. For all three scenarios, various degrees of difficulty in meeting the criticality limit, maximum peak pin power limit, and/or maximum peak pin discharge burnup limit were encountered. This was attributed to the more rapid decrease in assembly reactivity with burnup of LEU versus MOX assemblies, and LEU-MOX interfacial effects. The reactivity behavior with burnup effect produces a low average feed enrichment in the initial mixed LEU-MOX core. This implies less reactivity carry-forward in the subsequent cycle for the once burnt LEU assemblies, which is further aggravated at EOC by the fact that their reactivity decreases faster with burnup. Modification of the lattice design, which was restricted in this study to current ABB-CE LEU and MOX lattice designs, should be pursued to minimize the adverse LEU-MOX interfacial effects. To address the excessively high feed enrichments in subsequent cycles, it will likely be necessary to increase the number of feed assemblies to above that required to just satisfy the region average discharge burnup limit, the basis for the feed region size used in this study. Increasing feed region size should effectively address all the constraint violations, but at a considerable economic cost.

8. Acknowledgment

The authors would like to thank Dr. Trent Primm of Oak Ridge National Laboratory and Dr. Mark Kantrowitz of ABB-CE for their cooperation during the course of this study.

9. References

[1] "DOE Plutonium Disposition Study, Core Designs for Existing ABB-CE System 80 Reactors for the Disposition of Weapon-Grade Plutonium," Contract No. DE-AC03-93 SF-19682, ABB-Combustion Engineering (1996).

[2] "FMS: The Scanpower Fuel Management System, HELIOS Documentation," Scanpower A/S (1995).

[3] "FORMOSA-P V3.6.0 User's Manual: Fuel Management Optimization Software for PWRs," Electric Power Research Center, North Carolina State University (1998).

[4] "FORCIP-P Version 2.1 Code Manual: FORMOSA-P cross Section Interface Program," Electric Power Research Center, North Carolina State University (1998).

INTERNAL DISTRIBUTION

1. M. D. DeHart
2. R. J. Ellis
3. J. C. Gehin
4. S. R. Greene
5. S. A. Hodge
6. D. T. Ingersoll
7. M. A. Kuliasha
8. S. B. Ludwig
9. G. E. Michaels
10. D. L. Moses
11. B. D. Murphy
12. D. G. O'Connor
13–17. R. T. Primm III
18. C. C. Southmayd
19–23. D. J. Spellman
24. R. M. Westfall
25. K. A. Williams
26. B. A. Worley
27. Central Research Library
28. FMDP Library
29. ORNL Laboratory Records–RC

EXTERNAL DISTRIBUTION

30. M. L. Adams, Department of Nuclear Engineering, Texas A&M University, Zachry 129, College Station, TX 77843
31. Dave Alberstein, LANL, P.O. Box 1663, MS-K575, Los Alamos, NM 87545
32. G. Alonszo, Department of Nuclear Engineering, P.O. Box 7909, North Carolina State University, Raleigh, NC 27695-7909
33. Imelda Ariani, Department of Nuclear Engineering, P.O. Box 7909, North Carolina State University, Raleigh, NC 27695-7909
34. Tim Barr, DOE, Chicago Operations Office, 9700 S. Cass Avenue, Chicago, IL 60439
35. H. R. Canter, Office of Fissile Materials Disposition, Department of Energy, MD-1/2, 1000 Independence Avenue SW, Washington, DC 20585
36. G. S. Chang, INEEL, P.O. Box 1625, MS-3885, Idaho Falls, ID 83415-3885
37. A. I. Cygelman, Department of Energy, 1000 Independence A Avenue, SW, Forrestal Building 3F043, Washington, DC 20585
38. L. Groves, Sandia National Laboratories, P.O. Box 969, Livermore, CA 94551
39. D. Harrison, Department of Energy, 101 Convention Center Drive, Suite P200, Las Vegas, NV 89109
40. G. Holman, Lawrence Livermore National Laboratory, P.O. Box 808, Livermore, CA 94551
41. C. Jaeger, Sandia National Laboratories, P.O. Box 5800, Albuquerque, NM 78185-0759
42. Mark Kantrowitz, P.O. Box 500, 2000 Day Hill Road, Windsor, CT 06095-500
43. Frank Motley, LANL, P.O. Box 1663, MS-K575, Los Alamos, NM 87545

44–48. Office of the ORNL Site Manager, Department of Energy, Oak Ridge National Laboratory, P.O. Box 2008, Oak Ridge, TN 37831

49. D. Peko, Department of Energy, 1000 Independence Avenue, SW, Forrestal Building 3F042, Washington, DC 20585
50. P. T. Rhoads, Office of Fissile Materials Disposition, Department of Energy, MD-4, 1000 Independence Avenue SW, Washington, DC 20585
51. G. P. Rudy, Department of Energy, 1000 Independence Avenue, SW, Forrestal Building 7B192, Washington, DC 20585
52. J. M. Ryskamp, INEEL, P.O. Box 1625, MS-3885, Idaho Falls, ID 83415-3885
53. Robert Selby, Department of Energy, Chicago Operations Office, 9700 S. Cass Avenue, Chicago, IL 60439
54. J. Thompson, Office of Fissile Materials Disposition, Department of Energy, MD-4, 1000 Independence Avenue SW, Forrestal Building 3F043, Washington, DC 20585
55. Dr. Paul Turinsky, Department of Nuclear Engineering, North Carolina State University, Raleigh, NC 27695-7909